

1 Targeting NGF but not VEGF or BDNF signaling reduces

2 endometriosis-associated pain in mice

3 Tiago H. Zaninelli^{a,b}, Victor Fattori^a, Olivia K. Heintz^a, Kristenna R. Wright^a, Philip R.
4 Bennallack^a, Danielle Sim^a, Hussain Bukhari^a, Kathryn L. Terry^{c,d,e}, Allison F. Vitonis^{c,d}, Stacey
5 A. Missmer^{d,e,f}, Avacir C. Andrellog^g, Raymond M. Anchan^{d,h}, Stephen K. Godinⁱ, Dara Breeⁱ,
6 Waldiceu A. Verri Jr^b, Michael S. Rogers^{a,d*}

7

8 ^aVascular Biology Program, Department of Surgery, Boston Children's Hospital, Harvard Medical
9 School, Boston, MA, United States.

10 ^bLaboratory of Pain, Inflammation, Neuropathy, and Cancer, Department of Pathology, Center of
11 Biological Sciences, Londrina State University, Londrina, PR, Brazil.

12 ^cDepartment of Obstetrics, Gynecology, and Reproductive Biology, Brigham and Women's
13 Hospital and Harvard Medical School, Boston, MA, United States,

14 ^dBoston Center for Endometriosis, Boston Children's Hospital and Brigham and Women's
15 Hospital, Boston, MA, United States

16 ^eDepartment of Epidemiology, Harvard T.H. Chan School of Public Health, Boston, MA, United
17 States

18 ^fDepartment of Obstetrics, Gynecology, and Reproductive Biology, College of Human Medicine,
19 Michigan State University, Grand Rapids, MI, United States

20 ^gDepartment of Physics, Center of Exact Sciences, Londrina State University, Londrina, PR,
21 Brazil.

22 ^hDivision of Reproductive Endocrinology and Infertility, Department of Obstetrics, Gynecology
23 and Reproductive Biology, Brigham and Women's Hospital, Harvard Medical School, Boston,
24 MA, USA.

25 ⁱCygnal Therapeutics, Cambridge, MA, USA.

26 * Corresponding author

27 Address: Vascular Biology Program, Boston Children's Hospital, Department of Surgery,
28 Harvard Medical School, 11.211 Karp Family Research Bldg, 300 Longwood Ave, Boston,
29 MA 02115, United States. E-mail address: Michael.Rogers@childrens.harvard.edu (M.S.
30 Rogers).

31 Credit author statement

32

33

34 **Conceptualization:** T.H. Zaninelli, V. Fattori, and M.S. Rogers; **investigation and data**
35 **curation:** T.H. Zaninelli, V. Fattori, O.K. Heintz, K.R. Wright; A.C. Andrello, W.A. Verri Jr,
36 M.S. Rogers; **funding acquisition:** M.S. Rogers, , S.A. Missmer, R.M. Anchan; **methodology:**
37 T.H. Zaninelli, V. Fattori, and M.S. Rogers; **human sample collection:** S.A. Missmer, A.F.
38 Vitonis, K.L. Terry, R.M. Anchan; **animal breeding and VEGFR1 ablation:** D. Sim and H.
39 Bukhari; **resources:** A.C. Andrello; D. Bree, T. Zheng, J. Wagner, W.A. Verri Jr, and M.S. Rogers;
40 **project administration:** T.H. Zaninelli; **supervision:** V. Fattori, W.A. Verri Jr, and M.S. Rogers;
41 **visualization:** T.H. Zaninelli, V. Fattori, W.A. Verri Jr, and M.S. Rogers; **writing-original draft:**
42 T.H. Zaninelli; **writing – editing and reviewing:** all authors. All authors have read and approved
43 the final version of the manuscript.

44

45

46 **Abstract**

47

48 **Introduction:** Endometriosis is a chronic inflammatory disease that affects ~10% of women. A
49 significant fraction of patients experience limited or no efficacy with current therapies. Tissue
50 adjacent to endometriosis lesions often exhibits increased neurite and vascular density, suggesting
51 that disease pathology involves neurotrophic activity and angiogenesis.

52 **Objectives:** We aim to evaluate the potential for key tyrosine-kinase-receptor-coupled
53 neurotrophic molecules to contribute to endometriosis-associated pain in mice.

54 **Methods:** The levels of VEGFR1 regulators (VEGFA, VEGFB, PLGF, and sVEGFR1) were
55 quantified by ELISA in peritoneal fluid from endometriosis patients undergoing surgery and used
56 to calculate VEGFR1 occupancy. We used genetic depletion, neutralizing antibody, and
57 pharmacological approaches to specifically block ligand (NGF or BDNF) or neurotrophic receptor
58 (VEGFR1, TRKs) in a murine model of endometriosis-associated pain. Endometriosis-associated
59 pain was determined using the von Frey filaments method, quantification of spontaneous
60 abdominal pain-related behavior, and thermal discomfort. Disease parameters were evaluated by
61 lesion size and prevalence.

62 **Results:** We found that entrectinib (pan-Trk inhibitor) or anti-NGF treatments reduced evoked
63 pain, spontaneous pain, and thermal discomfort. In contrast, even though receptor occupancy
64 revealing that VEGFR1 agonist levels are sufficient to support pain, blocking VEGFR1 signaling
65 via antibody or tamoxifen-induced knockout did not reduce pain or lesion size in mice. Targeting
66 BDNF-TrkB with an anti-BDNF antibody also proved ineffective.

67 **Conclusions:** This suggests NGF-TrkA signaling, but not BDNF-TrkB or VEGF-VEGFR1,
68 mediates endometriosis-associated pain. Moreover, entrectinib blocks endometriosis-associated
69 pain and reduces lesion sizes. Our results also indicated that entrectinib-like molecules are
70 promising candidates for endometriosis treatment.

71

72 **Keywords:** neurotrophins; BDNF; VEGF; VEGFR1; visceral pain

73 **Introduction**

74 Endometriosis is an estrogen-dependent inflammatory disease characterized by the presence
75 of endometrium-like tissue in the abdominal cavity or pelvic space¹. The disease affects 10% of
76 people born with a uterus². The most studied pathway for endometriosis genesis is retrograde
77 menstruation³⁻⁵. During this process, danger-associated molecular patterns (DAMPs)⁶ activate
78 resident immune cells and trigger inflammation⁷. The inflammatory process is orchestrated by pro-
79 inflammatory mediators and growth factors secreted by activated immune cells^{7,8}. The growth-
80 factor-enriched inflammatory milieu favors angiogenesis and neurogenesis, resulting in
81 vascularized and innervated endometriotic lesions teeming with activated immune cells⁹. This
82 inflammation is key to pain, which is a prevalent clinical feature of those diagnosed with
83 endometriosis^{3,4}.

84 Endometriosis-associated pain appears as chronic pelvic pain, dysmenorrhea, dyspareunia, and
85 dyschezia, affecting the social and professional quality of life and mental health of patients with
86 endometriosis¹⁰. For instance, patients with endometriosis lose approximately 10 hours of work
87 weekly, because of reduced effectiveness during work due to endometriosis' symptoms¹¹.
88 Currently, endometriosis-associated pain treatment relies pharmaceutical and nonpharmaceutical
89 approaches including the use of non-steroidal anti-inflammatory drugs (NSAIDS), opiates and
90 other analgesics, hormonal therapy, pelvic therapy, acupuncture, and the surgical removal of
91 lesions¹². Nevertheless, current treatments show limited efficacy in reducing pain and often present
92 unwanted side effects¹³. Importantly, up to 30% of patients with endometriosis do not respond to
93 the current therapies¹⁴. Therefore, there is an unmet need to develop or repurpose effective and
94 safe drugs for the treatment of endometriosis-associated pain.

95 The endometriotic microenvironment is associated with increases in multiple tissue
96 remodeling growth factors, including nerve growth factor (NGF) and vascular endothelial growth
97 factor (VEGF), which are important mediators of neurogenesis and angiogenesis, respectively. In
98 addition to their growth-related role, those mediators are also described to be involved in pain^{15,16}.
99 Strong evidence shows that lesion growth is dependent on VEGFR2-mediated angiogenesis¹⁷⁻²⁰,
100 while VEGFR1 contributes to inflammatory milieu maintenance²¹. Moreover, VEGF has shown
101 promise in a panel of biomarker candidates for non-invasive endometriosis diagnosis²². In cancer
102 models, tumor-derived VEGF-A/B, and PIGF-2 increase pain sensitivity by activating VEGFR1¹⁶.
103 Similarly compelling evidence demonstrates that NGF might be involved in endometriosis pain²³.

104 High expression of *NGF* in deep adenomyotic nodules is correlated to hyperalgesia¹³ and both
105 *NGF* and *NTRK1* (TRKA) expression in human lesions correlate with deep dyspareunia in women
106 with endometriosis²⁴. Furthermore, a recent GWAS study showed that a variant in *NGF* is
107 associated with migraine and dysmenorrhea for women with endometriosis²⁵. However, the
108 relative contributions of various neurotrophic factors to endometriosis-associated pain remain
109 unclear.

110 To evaluate the effect of modulating cellular signaling of the neurotrophic molecules VEGF,
111 *NGF*, and BDNF as potential therapeutic targets for endometriosis-associated pain, we used our
112 validated mouse model of endometriosis. This model mimics neuronal and behavioral changes
113 consistent with the disease phenotype in women²⁶. Moreover, resulting lesions exhibit features that
114 resemble human lesions such as the presence of nerve fibers, glands, and immune cells. The model
115 responds to clinically active drugs, and therefore, might be useful for finding novel or repurposed
116 therapies²⁶.

117 **Materials and Methods**

118

119 *Patient samples*

120 Samples (n=33) of peritoneal fluid (PF) were collected and processed as part of the Women's
121 Health Study: From Adolescence to Adulthood (A2A) cohort²⁷. Samples were collected following
122 the WERF EPHect protocol²⁸ with some deviations. PF was housed in an incubator immediately
123 after collection until the specimen could be transported to the lab for processing. Samples were
124 centrifuged at 300g for 10 minutes at 4°C and frozen at -80°C using a Mr. Frosty freezing container.
125 Samples were kept frozen until aliquoting and only freeze-thawed twice. Additional samples (n=9)
126 were similarly collected following the WERF EPHect protocol from patients undergoing
127 exploratory laparoscopy surgery for endometriosis at Brigham and Women's Hospital (Boston,
128 MA, USA).

129

130 *Animals*

131 Healthy and immunologically competent C57BL/6 (8 weeks old, 20-25g, female, strain # 664
132 [RRID:IMSR_JAX:000664]), B6.Cg-Flt1^{tm1.1Fong}/J (8 weeks old, 20-25g, male and female, Vegfr-
133 1^{flx}, strain # 28098 [RRID:IMSR_JAX:028098]), and B6;129-Gt(ROSA)26Sor^{tm1(cre/ERT)Nat}/J (8
134 weeks old, 20-25g, male and female, R26CreER, strain # 4847 [RRID:IMSR_JAX:004847]) mice
135 were purchased from The Jackson Laboratory (Bar Harbor, Maine, USA). Vegfr-1^{flx} and
136 R26CreER were bred to generate tamoxifen-inducible Vegfr-1 knockout mice (Vegfr-
137 1^{flx/flx}R26CreER⁺⁻, Vegfr-1^{flx/flx}R26CreER⁺⁺), and littermate controls (Vegfr-
138 1^{flx/flx}R26CreER⁻). All mice were housed in standard clear cages with free access to food and
139 water. Controlled temperature (21°±1°C) and light/dark cycle of 12/12h. In all experiments, the
140 investigators were blinded to groups and treatments, including data acquisition, sample processing,
141 and data analyses. The animals were under isoflurane anesthesia (3% v/v in O₂) for endometriosis
142 induction, and tail snip sampling for genotyping. Carbon dioxide (CO₂) inhalation was used for
143 euthanasia. All efforts were made to minimize the number of animals and their suffering.

144

145 *Ethics statement*

146 All experiments involving animals were conducted according to the ethical policies and
147 procedures approved by the ethics committee of Boston Children's Hospital Institutional Animal

148 Care and Use Committee (IACUC, protocol number 19-12-4054R) and were in accordance with
149 the International Association for Study of Pain (IASP) and ARRIVE 2.0 guidelines.

150 All experiments involving human samples were also approved by Institutional Review Boards
151 (IRB). For samples from the Adolescence to Adulthood (A2A) cohort, the approval was conceived
152 by the Boston Children's Hospital IRB on behalf of Boston Children's Hospital and Brigham and
153 Women's Hospital. Informed consent was obtained, with parental consent/participant assent for
154 girls <18 years. The collection of additional samples was approved by the Mass General Brigham
155 IRB under protocol 2017P000184. Importantly, in both cases, sampling was performed only after
156 patients signed consent.

157

158 *Drugs and antibodies*

159 Tamoxifen (Sigma-Aldrich, cat# T5648), Entrectinib (InvivoChem, Libertyville, IL, USA,
160 CAS 1108743-60-7, cat# V0609); a mouse version of the rat anti-mouse VEGFR IgG1 antibody
161 MF1, (a kind gift from Eli Lilly & Co). anti-NGF (provided by Cygnal Therapeutics, Cambridge,
162 MA), anti-BDNF (provided by Cygnal Therapeutics), IgG control (anti-L1CAM provided by
163 Cygnal Therapeutics).

164

165 *Generation of VEGFR1 knockout mice*

166 VEGFR1 knockout was induced by tamoxifen treatment in Vegfr-1^{flox/flox}R26CreER⁺⁻ and
167 Vegfr-1^{flox/flox}R26CreER⁺⁺ mice. Littermate controls (Vegfr-1^{flox/flox}R26CreER^{-/-}) also received
168 the treatment. Mice were treated via oral gavage with Tamoxifen (6 mg/mouse/150 µL of corn oil)
169 every other day for 10 consecutive days. Endometriosis was induced 7 days after the last tamoxifen
170 administration. VEGFR1 KO was confirmed by genotyping and immunohistochemical staining of
171 the dorsal root ganglia (DRG).

172

173 *Induction of endometriosis*

174 A non-surgical model of endometriosis-associated pain was induced as previously
175 described²⁶. The mice were acclimatized at least one week before the experiment began. Donor
176 mice received a subcutaneous (s.c.) injection of 3 µg/mouse estradiol benzoate in sesame oil to
177 stimulate endometrium growth. Four to seven days later, the uteri from donor mice were dissected
178 and placed into a Petri dish containing Hank's Balanced Salt Solution (HBSS, Thermo Fisher

179 Scientific, Waltham, MA, USA). The uterine horns were split longitudinally with the aid of
180 scissors. The horns from each donor mouse were minced in consistent fragments smaller than 1
181 millimeter (mm). Each recipient mouse received a dissociated uterine horn in 500 μ L of HBSS
182 intraperitoneally for endometriosis induction. One donor mouse was used for every two
183 endometriosis mice. Sham mice received 500 μ L of HBSS intraperitoneally.

184

185 *Experimental design*

186 *Neurotrophic molecule signaling blockade*

187 We used two approaches to block VEGFR1 signaling in endometriosis: i) anti-VEGFR
188 monoclonal antibody and ii) VEGFR1 knockout (KO). Mice bearing endometriosis were treated
189 with a monoclonal antibody anti-VEGFR or IgG isotope (mMF1, 45 mg/kg) subcutaneously (s.c.),
190 twice a week starting 29 days post induction (29-56 d.p.i.). Mechanical hyperalgesia was assessed
191 weekly. In the last week of treatments (49 – 56 d.p.i.) spontaneous abdominal behavior and thermal
192 discomfort were quantified. On the 56th day mice were euthanized, and lesion size was
193 determined. In another set of experiments, VEGFR1 conditional knockout was performed in
194 CreER⁺ mice by tamoxifen administration (6 mg/animal) p.o. gavage every other day for 10 days.
195 To account for the effects of VEGFR1 in the tissue of donor and recipient mice, endometriosis was
196 induced in KO and littermate controls using uterine horns from KO or littermate control donor
197 mice, totaling 4 experimental groups. After endometriosis induction, mechanical hyperalgesia was
198 determined weekly using von Frey filaments. On the 56th d.p.i., lesions and DRG were harvested
199 for VEGFR1 KO confirmation by immunohistochemistry.

200 To target additional neurotrophin signaling two strategies were used: i) immunotherapy
201 using neutralizing antibodies anti-NGF and anti-BDNF, and ii) pharmacological treatment with
202 entrectinib a pan-selective inhibitor of tropomyosin receptor kinase (Trk) A, B, and C. Mice with
203 endometriosis were treated with antibodies anti-NGF, anti-BDNF, or IgG isotope (10 mg/kg)
204 subcutaneously (s.c.), twice a week beginning on day 29 post induction (29-56 d.p.i.). Mechanical
205 hyperalgesia was assessed weekly. In the last week of treatments (49 – 56 d.p.i.) spontaneous
206 abdominal behavior and thermal discomfort were quantified. Similarly, entrectinib was
207 administered by oral gavage in different treatment schedules to total 60 mg/kg/week per group.
208 Specifically, group 1 received entrectinib at 15 mg/kg every other day, group 2 at 20 mg/kg three
209 times a week, and group 3 at 60 mg/kg once a week. On the 56th day mice were euthanized, and

210 lesion size was determined. In the last week of treatments (49 – 56 d.p.i.) thermal discomfort was
211 assessed for all groups, while spontaneous abdominal behavior was quantified in group 3 (T3)
212 which received a single weekly treatment with 60 mg/kg. On the 56th day, lesions, blood, and
213 femur were harvested for lesion size determination, liver and kidney toxicity, and bone health
214 assessment, respectively.

215

216 *Determination of VEGFR1 ligand levels*

217 The concentrations of VEGFA, VEGFB, PIgf, and soluble VEGFR1 (sFL-1) were determined
218 by Ella Automated Immunoassay System according to manufacturer's instructions (ProteinSimple,
219 Bio-Techne, Minneapolis, MN, USA). VEGFR1 occupancy was calculated according to ligand-
220 receptor affinity, as previously described^{29–31}. The measurement of VEGF from mouse
221 endometriosis lesions was performed according to manufacturer's instructions using mouse VEGF
222 quantikine ELISA Kit (Cat# MMV00, R&D systems, Minneapolis, MN, USA).

223

224 *Immunostaining*

225 For VEGFR1 immunohistochemistry, the mouse dorsal root ganglia (DRG) were dissected 56
226 days after endometriosis induction and post-fixed in 4% paraformaldehyde in phosphate buffered
227 saline (PBS) (m/v) for 24h at room temperature (RT). Samples were dehydrated, paraffin
228 embedded, and sectioned in a microtome (Harvard Medical School Rodent Histology Core). The
229 7 µm thick sections were deparaffinized and hydrated before antigen retrieval in citrate buffer was
230 done. Slides were heated in a microwave until they reached 90°C and were cooled to RT.
231 Endogenous peroxidase was inactivated with 3% hydrogen peroxide in methanol (v/v) for 15 min
232 at RT. Sections were blocked in 3% bovine serum albumin (BSA) in PBS 0.5% triton-X 100
233 (m/v/v) for 1h at RT. Samples were incubated with rabbit anti-mouse VEGFR1 primary antibody
234 (Abcam, Cambridge, UK, cat# 32152, 1:200 dilution in PBS-T [RRID:AB_778798]) overnight at
235 4°C. Slides were washed and incubated with goat anti-rabbit-HRP secondary antibody for 30 min
236 at RT (Vector Laboratories, Newark, CA, USA, cat# MP-7451 [RRID:AB_2631198]). Color was
237 developed using HRP substrate kit (Vector Laboratories, cat# SK-4105 [RRID:AB_2336520]) for
238 1 min and 45 seconds at RT. Slides were washed and counterstained with Gills III Formulation
239 hematoxylin for 6 seconds, washed and dehydrated before slide mounting with PermountTM
240 mounting medium (Fisher Scientific, Waltham, MA, USA, cat# SP15-100).

241 For immunofluorescence analysis, mouse DRG and endometriotic lesions were dissected and
242 post-fixed in 4% paraformaldehyde in phosphate buffered saline (PBS) (m/v) for 24h at 4°C.
243 Samples were then dehydrated with 30% sucrose in PBS (m/v) for 48h at 4°C, followed by 30%
244 sucrose in PBS and optimum temperature cutting reagent (OCT) (1:1, v/v) for 24h at 4°C. DRG
245 and lesions were frozen in OCT, sectioned in a cryostat (16 μ m thick), and placed on silanized
246 slides. Sections were hydrated with PBS, blocked in 5% BSA in PBS 0.5% triton-X 100 (m/v/v)
247 for 1h at RT, following overnight incubation at 4°C with primary antibodies: mouse anti-mouse
248 phosphorylated-NF- κ B (pNF- κ B, Santa Cruz Biotechnology, Dallas, TX, USA, cat# sc-136548,
249 1:200 [RRID:AB_10610391]), rabbit anti-mouse TrkA (Invitrogen, Waltham MA, USA, cat. #
250 MA5-32123, 1:100 [RRID:AB_2809414]), rabbit anti-mouse NGF (Abcam, Boston, MA, USA,
251 cat. # AB52918, 1:300 [RRID:AB_881254]), and β -III tubulin (Novus Biologicals, Centennial,
252 CO, USA, cat. # NB120-11314, 1:200 [RRID:AB_792496]). Slices were then incubated with
253 appropriate secondary antibody: goat anti-mouse Alexa Fluor 594 secondary antibody (1:500, cat.
254 # A21125, Thermo Fisher Scientific [RRID:AB_141593]), goat anti-rabbit Alexa Fluor 647
255 secondary (1:500, cat. # A-21235, Thermo Fisher Scientific [RRID:AB_2535804]), or goat anti-
256 rabbit Alexa Fluor 488 (1:500, cat. # A-11008, Thermo Fisher Scientific [RRID:AB_143165]).
257 DAPI was used to stain nuclei (Cayman Chemicals, Ann Arbor, MI, USA, cat. # 14285). Images
258 were aquired and processed on a confocal microscope using 20x objective (Zeiss LSM 880 laser
259 scanning microscope with Airyscan, Carl Zeiss Microscopy, Thornwood, NY, USA).

260

261 *Animal behavior*

262 *Evoked abdominal mechanical hyperalgesia*

263 Mechanical hyperalgesia was assessed as previously described²⁶. Briefly, mice were
264 habituated to the conditions for at least 2h for three consecutive days before pain assessment. Pain
265 response to a mechanical stimulus (mechanical hyperalgesia) was measured using von Frey
266 filaments. Abdominal mechanical hyperalgesia was determined by a trained experimenter. The
267 area of external genitalia and consecutively stimulation in the same region were avoided. Jump or
268 paw flinches were considered as a withdrawal response³². The up-and-down method was used to
269 determine the mechanical threshold. Testing started with the 0.4g filament and measurements were
270 calculated using a modified version of the open-source software Up-Down Reader³³.

271

272 *Thermal gradient*

273 The thermal gradient assay was performed as previously described²⁶. Mice were placed on
274 a metallic base catwalk with a continuous temperature gradient (7–50 °C). Animals walked freely
275 while being video-recorded from above (Bioseb, France). Each run lasted 1.5 hours. After an
276 exploration period (30 minutes), the time mice spent in each temperature zone was recorded. Data
277 were presented as the time spent (in seconds) in each temperature zone during the last 60 minutes.

278

279 *Spontaneous pain behaviors*

280 Spontaneous abdominal pain was quantified using abdominal licking, stretching
281 (abdominal contortions), and squashing of the lower abdomen against the floor as previously
282 described²⁶. Direct abdominal licking was quantified for 10 minutes using bottom-up video
283 recording as the number of times (bouts) the mouse directly groomed the abdominal region without
284 going for any other region before or after the behavior. To measure abdominal contortions, mice
285 were placed in individual chambers and the number of abdominal contortions was quantified over
286 10 minutes. The computed behaviour consisted of abdominal muscle contraction in combination
287 with hind limbs stretch. Abdominal squashing, was quantified during 5 minutes, and the
288 considered behaviour was the number of times a mouse pressed its lower abdominal region against
289 the floor. In all testing, the investigators were blinded to the groups and treatments.

290

291 *Liver and kidney toxicity determination*

292 On the 56th d.p.i., mice were euthanatized, and their blood was collected into heparinized
293 collection tubes by cardiac puncture. Plasma was separated by centrifugation (3200 rpm, 10 min,
294 4°C). Kidney or liver toxicity was determined by the levels of urea, alanine aminotransferase
295 (ALT), and aspartate aminotransferase (AST) in the plasma. The levels were determined by
296 commercial kinetics kits according to manufacturer's instructions at the Longwood Small Animal
297 Imaging Facility (LSAIF) Blood lab at Beth Israel Deaconess Medical Center.

298

299 *Micro-computerized tomography analysis (µCT)*

300 The right femur was collected 56 days after endometriosis induction from entrectinib or vehicle
301 treated mice. Samples were fixed in paraformaldehyde 4% in PBS (m/v) for 24 h and maintained
302 in 70% ethanol (v/v) until µCT analysis. The samples were scanned on a Bruker SkyScan 1173

303 microtomograph (Bruker BioSpin Corporation, Kontich, Belgium). NRecon, DataViewer, CTvox,
304 and CTAn software was used to reconstruct and measure the images. The parameters analyzed
305 after image acquisition were bone surface, volume, density, total porosity, and open-pore volume.
306

307 *Statistical analysis*

308 Results are presented as mean \pm SEM. The data were analyzed using GraphPad Prism
309 version 8 (GraphPad Software, San Diego, CA, USA). Mechanical hyperalgesia was analyzed by
310 two-way repeated measure analysis of variance (ANOVA), followed by Tukey's *post hoc*. One-
311 way ANOVA followed by Tukey's *post hoc* was used to analyze data from experiments with a
312 single time point. Comparison between two groups was conducted using Student's t-test.

313 **Results**

314 Classical neurotrophins signal by binding to tyrosine kinase receptors to induce neurite
315 ingrown. The number of neurotrophic molecules and their receptor has steadily expanded since
316 the discovery of NGF and TrkA and VEGF signaling via VEGFR1 has been shown to have similar
317 effects. Therefore, we sought to evaluate the extent to which key neurotrophic molecules
318 contribute to endometriosis-associated pain.

319

320 *Levels of VEGFR1 ligands are increased in the peritoneal fluid of endometriosis patients and in*
321 *mouse lesions*

322 The role of VEGF signaling through VEGFR2 to induce angiogenesis has long been
323 recognized as a key means of supporting endometriosis lesion growth^{18,20,25,34,35}. However, the
324 potential for VEGFR1 activation to support neurite ingrowth has only been appreciated relatively
325 recently in the cancer context and has not been explored in endometriosis. Therefore, we first
326 measured the levels of VEGFR1 agonists in the peritoneal fluid of patients undergoing
327 endometriosis surgery (**Fig. 1 A-B**). We found that the concentrations of VEGFA, VEGFB, PIGF,
328 and sVEGFR1 were abundant in most evaluated samples (**Fig. 1B**). Based on the levels of
329 VEGFR1 agonists, the calculated VEGFR1 occupancy is sufficient to elicit neurite ingrowth and
330 thereby pain (**Fig. 1C**). Importantly, in peritoneal fluid, VEGFA concentrations were the major
331 driver of VEGFR1 occupancy, with log[VEGFA] predicting 90% of the variance.

332 To determine whether VEGFR1 signaling might also be present in our mouse model, we next
333 measured VEGFA levels in the mouse lesions. We demonstrated that VEGFA levels are increased
334 in endometriotic lesions (**Fig. 1E**) and that its receptor VEGFR1 is consistently expressed in DRG
335 neurons in naïve and endometriosis-bearing mice (**Fig. 1F**). Therefore, based in previous published
336 work¹⁶ and the present evidence, we hypothesized that VEGFR1 signaling might be important in
337 endometriosis-associated pain.

338

339 *VEGF neutralization or VEGFR1 ablation does not reduce endometriosis-associated pain or*
340 *thermal discomfort in mice*

341 To determine the extent to which VEGFR1 signaling is important for endometriosis-associated
342 pain, we targeted this signaling using two different strategies. First, we measured the extent to
343 which VEGFR1 neutralization with an anti-VEGFR1 monoclonal antibody (MF-1) would reduce

344 endometriosis-associated pain in mice. We found that treatment with anti-VEGFR1 did not alter
345 endometriosis-induced mechanical hyperalgesia (**Fig. 2B left**) or lesion size (**Fig. 2B right**). Since
346 spontaneous pain is the main complaint of patients with endometriosis, we next determined
347 whether treatment with MF-1 would reduce endometriosis-associated spontaneous pain. We found
348 that none of the spontaneous abdominal-related behaviors (licking, squashing, or contortions) were
349 reduced by the treatment (**Fig. 2C**). Finally, we assessed the mice's own determination of
350 discomfort using the thermal gradient assay. We confirmed that sham mice prefer temperatures 27
351 to 36 °C with a stronger preference for 34 °C, indicating that sham-treated mice were most
352 comfortable at that temperature. In contrast, mice with endometriosis exhibited a more dispersed
353 pattern ranging from 22 to 36 °C with no single preferred temperature, suggesting that lesion-
354 bearing mice were not comfortable at any temperature²⁶. In corroboration with our previous results,
355 blocking VEGF-VEGFR1 signaling did not reverse the loss of a comfort zone caused by lesions,
356 as demonstrated by the dispersed occupancy pattern in MF-1-treated mice (**Fig. 2D**). Since we
357 observed that treatment with anti-VEGFR1 did not reduce pain, we next wanted to establish the
358 extent to which VEGFR1 is required for the incitement of pain. Therefore, we first developed a
359 conditional tamoxifen-induced cre-dependent knockout mouse line (**Fig. 2E and F**). VEGFR1
360 floxed mice and littermate controls (LM) were treated with tamoxifen to induce cre-dependent
361 VEGFR1 gene ablation (**Fig. 2F**). Ablation of VEGFR1 expression was confirmed by
362 immunohistochemistry in the dorsal root ganglia (DRG) (**Fig. 2G**). We performed a four-group
363 experiment using VEGFR1-floxed and LM control mice as donors or recipients to determine the
364 extent to which the lack of VEGFR1 in donor tissue (mimicking retrograde menstruation) or in a
365 combination of donor and recipient play a role in endometriosis lesion formation and pain (**Fig.**
366 **2H left**). None of the investigated scenarios of VEGFR1 depletion demonstrated an analgesic
367 effect (**Fig. 2H right**). Therefore, while levels of VEGFR1 ligands are increased (both in humans
368 and mice), our data indicate that neither VEGFR1 in donor nor from recipient mice contribute to
369 endometriosis-associated pain.

370

371 *Entrectinib, a pan-Trk inhibitor, reduces endometriosis-associated pain and thermal discomfort*
372 *in mice*

373 Patients with endometriosis have higher levels of NGF in lesion as well as genetic variations
374 that correlates NGF to pain²⁵ indicating that NGF might play an important role in human

375 endometriosis pathology. Having found that VEGFR1 signaling does not contribute to pain in our
376 model and because NGF is often found in endometriosis lesions, we next sought to investigate
377 classical neurotrophins. To that end, we employed entrectinib, an inhibitor of the neurotrophin
378 receptors TrkA, TrkB, and TrkC. Entrectinib reduced mechanical hyperalgesia (**Fig. 3B left**) and
379 lesion size (**Fig. 3B right**) in all selected treatment schedules (T1 – T3) from day 42 to 56 post
380 endometriosis induction. Weekly delivery of entrectinib at 60 mg/kg was proven more effective in
381 restored comfort as measured in the thermal gradient when compared to vehicle treated mice (**Fig.**
382 **3C**). Since reduced and more frequent doses showed a milder reduction to thermal discomfort (T1
383 and T2), the weekly dose of 60 mg/kg was chosen for the next experiments (**Fig. 3C**). Because
384 spontaneous pain is the main symptom among patients with chronic pain, we determined the effect
385 of weekly treatment with entrectinib in spontaneous pain. We found that entrectinib-treated mice
386 showed reduced endometriosis-associated spontaneous behaviors (**Fig. 3D**). Altogether, our data
387 show that disruption in neurotrophin-Trk signaling is effective in reducing endometriosis-
388 associated pain.

389

390 *Neutralizing NGF, but not BDNF, reduces endometriosis-associated pain and thermal discomfort*
391 *in mice*

392 To determine the contribution of the Trk ligands NGF (TrkA) and BDNF (TrkB) in our
393 validated mouse model of endometriosis-associated pain, we then disrupted neurotrophin receptor
394 signaling. For that, we used neutralizing antibodies against NGF and BDNF. Upon measuring
395 mechanical hyperalgesia, lesion size, spontaneous behaviors, and thermal discomfort (**Fig. 4A**),
396 we observed that anti-NGF immunotherapy substantially reduced mechanical hyperalgesia from
397 the 42nd to 56th days after endometriosis induction (**Fig. 4B left**); other treatments were
398 ineffective. Although analgesic effects were maintained up to 56 d.p.i. in mice treated with anti-
399 NGF, no differences were observed in lesion size (**Fig. 4B right**). Based on these results, we next
400 analyzed spontaneous pain-associated behaviors and thermal discomfort only using anti-NGF
401 therapy (**Fig. 4C-D**). We found that the treatment with anti-NGF reduced endometriosis-induced
402 abdominal licking (**Fig. 4C left**) and squashing (**Fig. 4C middle**). A decrease in abdominal
403 contortions was also observed, however the difference vs. IgG-treated mice did not reach statistical
404 significance (**Fig. 4C right**). In the thermal gradient assay (**Fig. 4D**), anti-NGF therapy reduced
405 thermal discomfort, restoring the amplitude of time spent in specific thermal zones, when

406 compared to isotype-treated control mice (**fig. 4D**). Altogether, our results show that NGF-TrkA
407 signaling, but not BDNF-TrkB contributes to endometriosis-associate pain.

408

409 *NGF-TrkA signaling is activated during endometriosis*

410 To confirm that NGF's role in endometriosis pathogenesis²⁵ is accurately reflected in our
411 mouse model (**Fig. 5A**), we used immunofluorescence to stain for NGF in mouse lesions.
412 Interestingly, nociceptors seem to be closely located to this NGF gradient, as observed by
413 colocalization between NGF and β -tubulin III (TUJ3), a pan-neuronal marker (**Fig. 5B**). In the
414 DRG, lesion bearing mice displayed a higher percentage of TrkA-expressing neurons, and most
415 importantly, we found that TrkA⁺ nociceptors from mice with endometriosis demonstrated
416 increased activation as observed higher percentage of TrkA⁺pNF- κ B⁺ in comparison to sham (**Fig.**
417 **5C bottom, D**). Altogether, these data suggests that NGF-TrkA signaling is activated and might
418 contribute to pain in our model of endometriosis.

419

420 *Weekly treatment with entrectinib does not induce weight change, liver or kidney toxicity, or bone*
421 *loss in mice*

422 As mentioned, clinical trials with entrectinib in children and young adults demonstrated a high
423 incidence of bone fractures (clinicaltrials.gov, NCT02650401)³⁶. Given the generalized analgesic
424 effect of entrectinib with the different treatment schedules (**Fig. 3A, T1, T2, and T3**), we next
425 wanted to determine its safety. Even though the weekly dose proposed here is much lower than
426 the ones used in clinical trials, even after human equivalent dose determination, we sought to
427 determine kidney and liver function, and bone loss in mice (**Fig. 6A**). Weekly treatment with
428 entrectinib did not induce weight changes (**Fig. 6B**), nor kidney or liver function alteration as per
429 levels of urea (**Fig. 6C**), alanine aminotransferase (ALT) (**Fig. 6D Left**), or aspartate transaminase
430 (AST) (**Fig. 6D right**) in the plasma, respectively. Moreover, weekly treatment did not alter bone
431 parameters in the femur, as determined per micro-computerized tomography analysis (**Fig. 6E**).
432 No significant changes were observed in femur surface, volume, density, or porosity in the
433 evaluated dose and schedules of treatment. We found, however, that increasing number of
434 treatments, such as every other day (**Fig 6, T1**) or three times a week (**Fig 6, T2**), reduced bone
435 porosity (**Fig. 6E**). This indicates that while increased number of treatments with lower doses have

436 analgesic effects, this substantially affects bone porosity. This indicates that increased treatment
437 schedules, rather than dose, might be a limiting factor for entrectinib use.

438 **Discussion**

439 Pain is one of the key presenting symptoms of endometriosis. While pain correlates poorly
440 with lesion characteristics or rASRM-defined disease stage³⁷, peri-lesional TRPV1 staining
441 correlates with chronic pelvic pain^{38,39} and women with endometriosis-associated pain exhibit
442 dramatically increased nerve fiber densities^{40,41}. Lesion microvessel density is correlated with
443 pain⁴², suggesting that factors controlling both may play an important role in neurite recruitment.
444 NGF is a key neurotrophic factor²⁵ to maintaining TRPV1 neuronal expression^{43,44} and has long
445 been known to induce angiogenesis *in vivo*⁴⁵. In addition, when this work began, VEGF-A, acting
446 through VEGFR1 had recently been shown to modulate pain in the context of cancer by supporting
447 neuronal recruitment⁴⁶.

448 Prior to our work, it had already been shown that NGF is present at higher concentrations in
449 the peritoneal fluid of endometriosis patients vs. controls and that this results in increased
450 neurotrophic activity⁴⁷. It was also well-established that VEGF-A is upregulated in lesion tissue^{48–}
451 ⁵⁴ and peritoneal fluid^{55–64}, but the expression of other VEGFR1 ligands had not been explored.
452 We observed VEGFA, VEGFB, PlGF, and sVEGFR1 in the peritoneal fluid of patients undergoing
453 endometriosis surgery at levels that are more than sufficient to induce VEGFR1 activation and
454 signaling⁶⁵ and that VEGFA predominated in occupancy calculations. In our validated mouse
455 model²⁶, we found high levels of VEGF in the lesions as well as the presence of its receptor in
456 primary nociceptor neurons, suggesting a possible signaling axis to pain sensitivity. However,
457 blocking VEGFR1 signaling with anti-VEGFR1 antibody or cKO did not reduce pain or lesion
458 size. This indicates that while present in the lesion and peritoneal fluid, VEGF-VEGFR1 signaling
459 does not mediate pain in our model. Importantly, this model results in spontaneous pain, evoked
460 pain, and discomfort and these are alleviated by drugs known to alleviate pain in human patients²⁶.
461 These data suggest that anti-VEGFR1 treatment is unlikely to be effective in treating
462 endometriosis.

463 In contrast, we demonstrated that NGF/TrkA, but not BDNF/TrkB signaling, contributes to
464 endometriosis-related spontaneous and evoked pain responses. Blocking NGF signaling with
465 entrectinib, a pan-Trk inhibitor, reduced evoked abdominal mechanical pain as well as
466 spontaneous pain and discomfort. Specifically, we demonstrated that endometriosis-associated
467 pain is mediated via NGF-TrkA signaling, since blocking NGF with an antibody reduced pain to
468 approximately the same extent as entrectinib, while blocking BDNF signaling had no effect on

469 pain, notwithstanding the expected effect on mouse body weight. The fact that anti-NGF and
470 entrectinib treatment had similar effect sizes also suggests, but does not prove, that TrkC ligands
471 may have little effect in our model.

472 This observation is consistent with literature showing that neurotrophic factors, such as NGF,
473 participate in inflammatory pain⁶⁶ and neuropathic pain⁶⁷. NGF contributes both indirectly and
474 directly to nociceptor neuron sensitization and pain. NGF signaling via TrkA in immune cells (e.g.,
475 mast cells, basophils, macrophages)⁶⁸⁻⁷⁰ results in the release of NGF and other pro-nociceptive
476 molecules, such as interleukin (IL)-1 β ⁷¹. NGF also directly induces nociceptor neurons
477 sensitization and activation¹⁵. Specifically for endometriosis, a recent GWAS study highlighted
478 that variance among genes such as NGF is associated with pain presentation²⁵. Therefore, we
479 hypothesized that neurotrophins (e.g., NGF and BDNF) participate in endometriosis-associated
480 pain. Our data show that NGF is co-localized with TUJ3 in endometriosis and that TrkA⁺ DRG
481 neurons are activated during endometriosis. This corroborates human findings that show both NGF
482 and TrkA are highly expressed in endometriosis lesions and are correlated with nerve fiber density
483 and deep dyspareunia⁴⁷. In corroboration, we found that anti-NGF immunotherapy reduced
484 endometriosis-associated evoked and spontaneous pain behaviors in mice. Anti-NGF treatment
485 reduced mechanical hyperalgesia, abdominal licking, squashing, and contortions, and decreased
486 thermal discomfort. Similarly, in a model of cyclophosphamide-induced cystitis, treatment with
487 anti-NGF reduces peripheral hypersensitivity in mice⁷². Pain inhibition was also observed in the
488 same model of cystitis in rats when animals were treated with the NGF sequestering protein
489 REN1820⁷³. Humanized anti-NGF monoclonal antibodies have been clinically tested in
490 osteoarthritis⁷⁴⁻⁷⁷, low back pain⁷⁸, diabetes-associated neuropathy⁷⁹, and interstitial cystitis⁸⁰,
491 corroborating the observed phenomena. On the other hand, we found that anti-BDNF
492 immunotherapy did not reduce any of the evaluated parameters. Altogether, this indicates that
493 NGF-TrkA signaling, but not BDNF-TrkB, mediates endometriosis-associated pain in our model.

494 Herein, we demonstrated weekly treatments with low doses of entrectinib (60 mg/kg) reduced
495 evoked and non-evoked pain behaviors in mice. This suggests that discontinuous disruption of
496 NGF-TrkA signaling, by weekly treatments with entrectinib, is sufficient to decrease
497 endometriosis-associated pain. This effect is likely to be via NGF-TrkA signaling since pain
498 (evoked and spontaneous) in our model was reduced after treatment with anti-NGF, but not anti-
499 BDNF. In this context, it is worth noting that NGF targeting therapies are often linked to undesired

500 side effects. Of greatest concern, while all studies show that anti-NGF decreases pain, in a portion
501 of patients with osteoarthritis, anti-NGF therapy was correlated to joint destruction and the need
502 for total joint replacement²⁵. Similarly, treatments with entrectinib in children and young adults
503 increased the incidence of bone fractures (clinicaltrials.gov, NCT02650401)³⁶. Based on the
504 clinical relevance of NGF-targeting treatment for endometriosis pain management, we addressed
505 the safety of entrectinib in the dose and schedule of treatments tested in this study. Herein, we
506 demonstrated that weekly treatment with entrectinib at 60 mg/kg did not induce changes in weight
507 gain, liver, or kidney toxicity, nor bone morphology. Therefore, in this pre-clinical study, we found
508 that discontinuous low doses of entrectinib reduced endometriosis-associated pain while not
509 showing significant side effects.

510

511 **Conclusion**

512 In this study we demonstrated that while VEGFR1 agonists are upregulated in the peritoneal
513 fluid of women with endometriosis, blocking this signaling does not reduce pain in a murine
514 model. On the other hand, we found that the neurotrophin NGF (but not BDNF) is key for
515 endometriosis-associated pain. Blocking this signaling with anti-NGF or entrectinib is effective at
516 reducing abdominal mechanical pain, spontaneous pain, and thermal discomfort in our model.
517 Moreover, weekly treatments with entrectinib did not show significant side effects in mice. The
518 lack of drug efficacy at reducing ongoing pain drives most endometriosis therapy failure.
519 Therefore, our study pinpoints NGF as a key factor in endometriosis-associated pain and
520 establishes NGF-TrkA signaling as a potential target for the development of novel therapies for
521 endometriosis.

522

523 **Funding**

524 This work was supported by grants from The J. Willard and Alice S. Marriott Foundation
525 and Marriott Daughters Foundation.

526

527 **Acknowledgments**

528 T.H.Z. acknowledges international split PhD scholarship (*Programa de Doutorado*
529 *Sanduiche no Exterior – PDSE*) from Coordination for the Improvement of Higher Education
530 Personnel (CAPES, Brazil, finance code 001). We also thank the support of Multiuser Center for
531 Research Laboratories of Londrina State University for the access to μ CT equipment free of
532 charge. W.A.V.J. acknowledges CNPq fellowship (#309633/2021-4). We are also thankful for the
533 collaboration of Rachel Arredondo for English editing this manuscript.

534

535 **Declaration of interests**

536 The authors declare no conflicts of interest.

537 **References**

- 538 1. Zondervan, K.T., Becker, C.M., and Missmer, S.A. (2020). Endometriosis. *N Engl J Med*
539 382, 1244–1256. 10.1056/NEJMra1810764.
- 540 2. Parasar, P., Ozcan, P., and Terry, K.L. (2017). Endometriosis: Epidemiology, Diagnosis
541 and Clinical Management. *Curr Obstet Gynecol Rep* 6, 34–41. 10.1007/S13669-017-
542 0187-1/TABLES/2.
- 543 3. Laux-Biehlmann, A., d'Hooghe, T., and Zollner, T.M. (2015). Menstruation pulls the
544 trigger for inflammation and pain in endometriosis. *Trends Pharmacol Sci* 36, 270–276.
545 10.1016/j.tips.2015.03.004.
- 546 4. McKinnon, B.D., Bertschi, D., Bersinger, N.A., and Mueller, M.D. (2015). Inflammation
547 and nerve fiber interaction in endometriotic pain. *Trends Endocrinol Metab* 26, 1–10.
548 10.1016/j.tem.2014.10.003.
- 549 5. Bulun, S.E., Yildiz, S., Adli, M., Chakravarti, D., Parker, J.B., Milad, M., Yang, L.,
550 Chaudhari, A., Tsai, S., Wei, J.J., et al. (2023). Endometriosis and adenomyosis: shared
551 pathophysiology. *Fertil Steril* 119, 746–750. 10.1016/J.FERTNSTERT.2023.03.006.
- 552 6. Patel, S. (2018). Danger-Associated Molecular Patterns (DAMPs): the Derivatives and
553 Triggers of Inflammation. *Curr Allergy Asthma Rep* 18. 10.1007/S11882-018-0817-3.
- 554 7. Izumi, G., Koga, K., Takamura, M., Makabe, T., Satake, E., Takeuchi, A., Taguchi, A.,
555 Urata, Y., Fujii, T., and Osuga, Y. (2018). Involvement of immune cells in the
556 pathogenesis of endometriosis. *Journal of Obstetrics and Gynaecology Research* 44, 191–
557 198. 10.1111/jog.13559.
- 558 8. Wu, J., Xie, H., Yao, S., and Liang, Y. (2017). Macrophage and nerve interaction in
559 endometriosis. *J Neuroinflammation* 14, 53. 10.1186/s12974-017-0828-3.
- 560 9. Abramiuk, M., Grywalska, E., Małkowska, P., Sierawska, O., Hrynkiewicz, R., and
561 Niedźwiedzka-Rystwej, P. (2022). The Role of the Immune System in the Development of
562 Endometriosis. *Cells* 11. 10.3390/CELLS11132028.
- 563 10. Facchini, F., Barbara, G., Saita, E., Mosconi, P., Roberto, A., Fedele, L., and Vercellini, P.
564 (2015). Impact of endometriosis on quality of life and mental health: pelvic pain makes
565 the difference. *J Psychosom Obstet Gynaecol* 36, 135–141.
566 10.3109/0167482X.2015.1074173.
- 567 11. Nnoaham, K.E., Hummelshoj, L., Webster, P., D'Hooghe, T., De Cicco Nardone, F., De
568 Cicco Nardone, C., Jenkinson, C., Kennedy, S.H., and Zondervan, K.T. (2011). Impact of
569 endometriosis on quality of life and work productivity: A multicenter study across ten
570 countries. *Fertil Steril* 96. 10.1016/j.fertnstert.2011.05.090.
- 571 12. Horne, A.W., and Missmer, S.A. (2022). Pathophysiology, diagnosis, and management of
572 endometriosis. *BMJ* 379. 10.1136/BMJ-2022-070750.
- 573 13. Anaf, V., Simon, P., El Nakadi, I., Fayt, I., Simonart, T., Buxant, F., and Noel, J.C.
574 (2002). Hyperalgesia, nerve infiltration and nerve growth factor expression in deep
575 adenomyotic nodules, peritoneal and ovarian endometriosis. *Hum Reprod* 17, 1895–1900.
576 10.1093/HUMREP/17.7.1895.
- 577 14. Becker, C.M., Gattrell, W.T., Gude, K., and Singh, S.S. (2017). Reevaluating response
578 and failure of medical treatment of endometriosis: a systematic review. *Fertil Steril* 108,
579 125–136. 10.1016/J.FERTNSTERT.2017.05.004.
- 580 15. Bonnington, J.K., and McNaughton, P.A. (2003). Signalling pathways involved in the
581 sensitisation of mouse nociceptive neurones by nerve growth factor. *J Physiol* 551, 433.
582 10.1113/JPHYSIOL.2003.039990.

583 16. Selvaraj, D., Gangadharan, V., Michalski, C.W., Kurejova, M., Stosser, S., Srivastava, K.,
584 Schweizerhof, M., Waltenberger, J., Ferrara, N., Heppenstall, P., et al. (2015). A
585 Functional Role for VEGFR1 Expressed in Peripheral Sensory Neurons in Cancer Pain.
586 *Cancer Cell* 27, 780–796. 10.1016/j.ccr.2015.04.017.

587 17. Xavier, P., Belo, L., Beires, J., Rebelo, I., Martinez-de-Oliveira, J., Lunet, N., and Barros,
588 H. (2006). Serum levels of VEGF and TNF-alpha and their association with C-reactive
589 protein in patients with endometriosis. *Arch Gynecol Obstet* 273, 227–231.
590 10.1007/S00404-005-0080-4.

591 18. Yildiz, C., Kacan, T., Akkar, O.B., Karakus, S., Kacan, S.B., Ozer, H., and Cetin, A.
592 (2015). Effects of Pazopanib, Sunitinib, and Sorafenib, Anti-VEGF Agents, on the Growth
593 of Experimental Endometriosis in Rats. *Reprod Sci* 22, 1445–1451.
594 10.1177/1933719115584448.

595 19. Ozer, H., Boztosun, A., Aćmaz, G., Atilgan, R., Akkar, O.B., and Kosar, M.I. (2013). The
596 efficacy of bevacizumab, sorafenib, and retinoic acid on rat endometriosis model. *Reprod
597 Sci* 20, 26–32. 10.1177/1933719112452941.

598 20. Leconte, M., Santulli, P., Chouzenoux, S., Marcellin, L., Cerles, O., Chapron, C., Dousset,
599 B., and Batteux, F. (2015). Inhibition of MAPK and VEGFR by Sorafenib Controls the
600 Progression of Endometriosis. *Reprod Sci* 22, 1171–1180. 10.1177/1933719115592708.

601 21. Sekiguchi, K., Ito, Y., Hattori, K., Inoue, T., Hosono, K., Honda, M., Numao, A., Amano,
602 H., Shibuya, M., Unno, N., et al. (2019). VEGF Receptor 1-Expressing Macrophages
603 Recruited from Bone Marrow Enhances Angiogenesis in Endometrial Tissues. *Sci Rep* 9.
604 10.1038/S41598-019-43185-8.

605 22. Vodolazkaia, A., El-Aalamat, Y., Popovic, D., Mihalyi, A., Bossuyt, X., Kyama, C.M.,
606 Fassbender, A., Bokor, A., Schols, D., Huskens, D., et al. (2012). Evaluation of a panel of
607 28 biomarkers for the non-invasive diagnosis of endometriosis. *Hum Reprod* 27, 2698–
608 2711. 10.1093/HUMREP/DES234.

609 23. Kajitani, T., Maruyama, T., Asada, H., Uchida, H., Oda, H., Uchida, S., Miyazaki, K.,
610 Arase, T., Ono, M., and Yoshimura, Y. (2013). Possible involvement of nerve growth
611 factor in dysmenorrhea and dyspareunia associated with endometriosis. *Endocr J* 60,
612 1155–1164. 10.1507/ENDOCRJ.EJ13-0027.

613 24. Peng, B., Zhan, H., Alotaibi, F., Alkusayer, G.M., Bedaiwy, M.A., and Yong, P.J. (2018).
614 Nerve Growth Factor Is Associated With Sexual Pain in Women With Endometriosis.
615 *Reproductive Sciences* 25, 540–549. 10.1177/1933719117716778.

616 25. Rahmioglu, N., Mortlock, S., Ghiasi, M., Møller, P.L., Stefansdottir, L., Galarneau, G.,
617 Turman, C., Danning, R., Law, M.H., Sapkota, Y., et al. (2023). The genetic basis of
618 endometriosis and comorbidity with other pain and inflammatory conditions. *Nat Genet*
619 55, 423–436. 10.1038/S41588-023-01323-Z.

620 26. Fattori, V., Franklin, N.S., Gonzalez-Cano, R., Peterse, D., Ghalali, A., Madrian, E., Verri,
621 W.A., Andrews, N., Woolf, C.J., and Rogers, M.S. (2020). Nonsurgical mouse model of
622 endometriosis-associated pain that responds to clinically active drugs. *Pain* 161, 1321–
623 1331. 10.1097/J.PAIN.0000000000001832.

624 27. Sasamoto, N., Shafrir, A.L., Wallace, B.M., Vitonis, A.F., Fraer, C.J., Sadler Gallagher, J.,
625 Depari, M., Ghiasi, M., Laufer, M.R., Sieberg, C.B., et al. (2023). Trends in pelvic pain
626 symptoms over 2 years of follow-up among adolescents and young adults with and
627 without endometriosis. *Pain* 164, 613–624. 10.1097/J.PAIN.0000000000002747.

628 28. Rahmioglu, N., Fassbender, A., Vitonis, A.F., Tworoger, S.S., Hummelshoj, L.,
629 D'Hooghe, T.M., Adamson, G.D., Giudice, L.C., Becker, C.M., Zondervan, K.T., et al.
630 (2014). World Endometriosis Research Foundation Endometriosis Phenome and
631 Biobanking Harmonization Project: III. Fluid biospecimen collection, processing, and
632 storage in endometriosis research. *Fertil Steril* 102, 1233–1243.
633 10.1016/J.FERTNSTERT.2014.07.1208.

634 29. Anisimov, A., Leppänen, V.M., Tvorogov, D., Zarkada, G., Jeltsch, M., Holopainen, T.,
635 Kaijalainen, S., and Alitalo, K. (2013). The basis for the distinct biological activities of
636 vascular endothelial growth factor receptor-1 ligands. *Sci Signal* 6.
637 10.1126/SCISIGNAL.2003905/SUPPL_FILE/6_RA52_SM.PDF.

638 30. Fischer, C., Mazzone, M., Jonckx, B., and Carmeliet, P. (2008). FLT1 and its ligands
639 VEGFB and PIGF: drug targets for anti-angiogenic therapy? *Nature Reviews Cancer* 2008
640 8:12 8, 942–956. 10.1038/nrc2524.

641 31. Wu, F.T.H., Stefanini, M.O., Mac Gabhann, F., and Popel, A.S. (2009). A Compartment
642 Model of VEGF Distribution in Humans in the Presence of Soluble VEGF Receptor-1
643 Acting as a Ligand Trap. *PLoS One* 4, e5108. 10.1371/JOURNAL.PONE.0005108.

644 32. Gonzalez-Cano, R., Merlos, M., Baeyens, J.M., and Cendan, C.M. (2013). sigma1
645 receptors are involved in the visceral pain induced by intracolonic administration of
646 capsaicin in mice. *Anesthesiology* 118, 691–700. 10.1097/ALN.0b013e318280a60a.

647 33. Gonzalez-Cano, R., Boivin, B., Bullock, D., Cornelissen, L., Andrews, N., and Costigan, M. (2018). Up-Down reader: An open source program for efficiently processing 50% von
648 frey thresholds. *Front Pharmacol* 9. 10.3389/fphar.2018.00433.

649 34. Fallon, E.M., Nehra, D., Carlson, S.J., Potemkin, A.K., Mitchell, P.D., Nedder, A.P.,
650 Rueda, B.R., and Puder, M. (2012). Sunitinib reduces recurrent pelvic adhesions in a
651 rabbit model. *J Surg Res* 178, 860–865. 10.1016/J.JSS.2012.07.038.

652 35. Kim, S., Lee, S., Greene, A.K., Arsenault, D.A., Le, H., Meisel, J., Novak, K., Flynn, E.,
653 Heymach, J. V., and Puder, M. (2008). Inhibition of intra-abdominal adhesion formation
654 with the angiogenesis inhibitor sunitinib. *J Surg Res* 149, 115–119.
655 10.1016/J.JSS.2007.10.010.

656 36. Desai, A. V, Robinson, G.W., Gauvain, K., Basu, E.M., Macy, M.E., Maese, L., Whipple,
657 N.S., Sabnis, A.J., Foster, J.H., Shusterman, S., et al. (2022). Entrectinib in children and
658 young adults with solid or primary CNS tumors harboring NTRK, ROS1, or ALK
659 aberrations (STARTRK-NG). *Neuro Oncol* 24. 10.1093/NEUONC/NOAC087.

660 37. Parasar, P., Ozcan, P., and Terry, K.L. (2017). Endometriosis: Epidemiology, Diagnosis
661 and Clinical Management. *Curr Obstet Gynecol Rep* 6, 34. 10.1007/S13669-017-0187-1.

662 38. Rocha, M.G., e Silva, J.C., Ribeiro da Silva, A., Candido Dos Reis, F.J., Nogueira, A.A.,
663 and Poli-Neto, O.B. (2011). TRPV1 expression on peritoneal endometriosis foci is
664 associated with chronic pelvic pain. *Reprod Sci* 18, 511–515.
665 10.1177/1933719110391279.

666 39. Poli-Neto, O.B., Filho, A.A., Rosa e Silva, J.C., Barbosa Hde, F., Candido Dos Reis, F.J.,
667 and Nogueira, A.A. (2009). Increased capsaicin receptor TRPV1 in the peritoneum of
668 women with chronic pelvic pain. *Clin J Pain* 25, 218–222.
669 10.1097/AJP.0b013e318188378a.

670 40. Tran, L.V.P., Tokushige, N., Berbic, M., Markham, R., and Fraser, I.S. (2009).
671 Macrophages and nerve fibres in peritoneal endometriosis. *Human Reproduction* 24, 835–
672 841. 10.1093/humrep/den483.

673

674 41. Tokushige, N., Markham, R., Russell, P., and Fraser, I.S. (2006). High density of small
675 nerve fibres in the functional layer of the endometrium in women with endometriosis.
676 *Hum Reprod* *21*, 782–787. 10.1093/HUMREP/DEI368.

677 42. García-Manero, M., Santana, G.T., and Alcázar, J.L. (2008). Relationship between
678 microvascular density and expression of vascular endothelial growth factor in patients
679 with ovarian endometriosis. *J Womens Health (Larchmt)* *17*, 777–782.
680 10.1089/JWH.2007.0695.

681 43. Winter, J., Alistair Forbes, C., Sternberg, J., and Lindsay, R.M. (1988). Nerve growth
682 factor (NGF) regulates adult rat cultured dorsal root ganglion neuron responses to the
683 excitotoxin capsaicin. *Neuron* *1*, 973–981. 10.1016/0896-6273(88)90154-7.

684 44. Bevan, S., and Winter, J. (1995). Nerve growth factor (NGF) differentially regulates the
685 chemosensitivity of adult rat cultured sensory neurons. *Journal of Neuroscience* *15*, 4918–
686 4926. 10.1523/JNEUROSCI.15-07-04918.1995.

687 45. Santos, P.M., Winterowd, J.G., Allen, G.G., Bothwell, M.A., and Rubel, E.W. (1991).
688 Nerve growth factor: increased angiogenesis without improved nerve regeneration.
689 *Otolaryngol Head Neck Surg* *105*, 12–25. 10.1177/019459989110500103.

690 46. Selvaraj, D., Gangadharan, V., Michalski, C.W., Kurejova, M., Stosser, S., Srivastava, K.,
691 Schweizerhof, M., Waltenberger, J., Ferrara, N., Heppenstall, P., et al. (2015). A
692 Functional Role for VEGFR1 Expressed in Peripheral Sensory Neurons in Cancer Pain.
693 *Cancer Cell* *27*, 780–796. 10.1016/j.ccr.2015.04.017.

694 47. Barcena De Arellano, M.L., Arnold, J., Vercellino, F., Chiantera, V., Schneider, A., and
695 Mechsner, S. (2011). Overexpression of nerve growth factor in peritoneal fluid from
696 women with endometriosis may promote neurite outgrowth in endometriotic lesions. *Fertil*
697 *Steril* *95*, 1123–1126. 10.1016/J.FERTNSTERT.2010.10.023.

698 48. Zhang, L., Xiong, W., Xiong, Y., Liu, H., and Liu, Y. (2016). 17 β -Estradiol promotes
699 vascular endothelial growth factor expression via the Wnt/ β -catenin pathway during the
700 pathogenesis of endometriosis. *Mol Hum Reprod* *22*, 526–535.
701 10.1093/MOLEHR/GAW025.

702 49. Oliveira, V.A., Abreu, L.G., Ferriani, R.A., Reis, R.M., and Moura, M.D. (2005).
703 Vascular endothelial growth factor in the plasma, follicular fluid and granulosa cells of
704 women with endometriosis submitted to in vitro fertilization--a pilot study. *Gynecol*
705 *Endocrinol* *20*, 284–288. 10.1080/09513590500097952.

706 50. Machado, D.E., Abrao, M.S., Berardo, P.T., Takiya, C.M., and Nasciutti, L.E. (2008).
707 Vascular density and distribution of vascular endothelial growth factor (VEGF) and its
708 receptor VEGFR-2 (Flk-1) are significantly higher in patients with deeply infiltrating
709 endometriosis affecting the rectum. *Fertil Steril* *90*, 148–155.
710 10.1016/J.FERTNSTERT.2007.05.076.

711 51. Di Carlo, C., Bonifacio, M., Tommaselli, G.A., Bifulco, G., Guerra, G., and Nappi, C.
712 (2009). Metalloproteinases, vascular endothelial growth factor, and angiopoietin 1 and 2
713 in eutopic and ectopic endometrium. *Fertil Steril* *91*, 2315–2323.
714 10.1016/J.FERTNSTERT.2008.03.079.

715 52. Van Den Berg, L.L., Crane, L.M.A., Van Oosten, M., Van Dam, G.M., Simons, A.H.M.,
716 Hofker, H.S., and Bart, J. (2013). Analysis of biomarker expression in severe
717 endometriosis and determination of possibilities for targeted intraoperative imaging. *Int J*
718 *Gynaecol Obstet* *121*, 35–40. 10.1016/J.IJGO.2012.10.025.

719 53. Tan, C.W., Lee, Y.H., Tan, H.H., Lau, M.S.K., Choolani, M., Griffith, L., and Chan, J.K.Y. (2014). CD26/DPPIV down-regulation in endometrial stromal cell migration in endometriosis. *Fertil Steril* 102. 10.1016/J.FERTNSTERT.2014.04.001.

720 54. Braza-Boïls, A., Marí-Alexandre, J., Gilabert, J., Sánchez-Izquierdo, D., España, F., Estellés, A., and Gilabert-Estellés, J. (2014). MicroRNA expression profile in endometriosis: its relation to angiogenesis and fibrinolytic factors. *Hum Reprod* 29, 978–988. 10.1093/HUMREP/DEU019.

721 55. Cho, S.H., Choi, Y.S., Jeon, Y.E., Im, K.J., Choi, Y.M., Yim, S.Y., Kim, H.Y., Seo, S.K., and Lee, B.S. (2012). Expression of vascular endothelial growth factor (VEGF) and its soluble receptor-1 in endometriosis. *Microvasc Res* 83, 237–242. 10.1016/J.MVR.2011.12.004.

722 56. Shifren, J.L., Tseng, J.F., Zaloudek, C.J., Ryan, I.P., Meng, Y.G., Ferrara, N., Jaffe, R.B., and Taylor, R.N. (1996). Ovarian steroid regulation of vascular endothelial growth factor in the human endometrium: implications for angiogenesis during the menstrual cycle and in the pathogenesis of endometriosis. *J Clin Endocrinol Metab* 81, 3112–3118. 10.1210/JCEM.81.8.8768883.

723 57. McLaren, J., Prentice, A., Charnock-Jones, D.S., and Smith, S.K. (1996). Vascular endothelial growth factor (VEGF) concentrations are elevated in peritoneal fluid of women with endometriosis. *Hum Reprod* 11, 220–223. 10.1093/OXFORDJOURNALS.HUMREP.A019023.

724 58. McLaren, J., Prentice, A., Charnock-Jones, D.S., Millican, S.A., Müller, K.H., Sharkey, A.M., and Smith, S.K. (1996). Vascular endothelial growth factor is produced by peritoneal fluid macrophages in endometriosis and is regulated by ovarian steroids. *J Clin Invest* 98, 482–489. 10.1172/JCI118815.

725 59. Mahnke, J.L., Yusoff Dawood, M., and Huang, J.C. (2000). Vascular endothelial growth factor and interleukin-6 in peritoneal fluid of women with endometriosis. *Fertil Steril* 73, 166–170. 10.1016/S0015-0282(99)00466-5.

726 60. Na, Y.J., Yang, S.H., Baek, D.W., Lee, D.H., Kim, K.H., Choi, Y.M., Oh, S.T., Hong, Y.S., Kwak, J.Y., and Lee, K.S. (2006). Effects of peritoneal fluid from endometriosis patients on the release of vascular endothelial growth factor by neutrophils and monocytes. *Hum Reprod* 21, 1846–1855. 10.1093/HUMREP/DEL077.

727 61. Wang, H., Gorpudolo, N., Li, Y., Feng, D., Wang, Z., and Zhang, Y. (2009). Elevated vascular endothelia growth factor-A in the serum and peritoneal fluid of patients with endometriosis. *J Huazhong Univ Sci Technolog Med Sci* 29, 637–641. 10.1007/S11596-009-0520-7.

728 62. Bourlev, V., Iljasova, N., Adamyan, L., Larsson, A., and Olovsson, M. (2010). Signs of reduced angiogenic activity after surgical removal of deeply infiltrating endometriosis. *Fertil Steril* 94, 52–57. 10.1016/J.FERTNSTERT.2009.02.019.

729 63. Kianpour, M., Nematbakhsh, M., Ahmadi, S.M., Jafarzadeh, M., Hajjarian, M., Pezeshki, Z., Safari, T., and Eshraghi-Jazi, F. (2013). Serum and peritoneal fluid levels of vascular endothelial growth factor in women with endometriosis. *Int J Fertil Steril* 7, 96–99.

730 64. Szubert, M., Suzin, J., Duechler, M., Szuławska, A., Czyz, M., and Kowalczyk-Amico, K. (2014). Evaluation of selected angiogenic and inflammatory markers in endometriosis before and after danazol treatment. *Reprod Fertil Dev* 26, 414–420. 10.1071/RD12258.

731 65. Clauss, M., Weich, H., Breier, G., Knies, U., Röckl, W., Waltenberger, J., and Risaut, W. (1996). The vascular endothelial growth factor receptor Flt-1 mediates biological

765 activities. Implications for a functional role of placenta growth factor in monocyte
766 activation and chemotaxis. *J Biol Chem* 271, 17629–17634. 10.1074/JBC.271.30.17629.

767 66. Woolf, C.J., Safieh-Garabedian, B., Ma, Q.P., Crilly, P., and Winter, J. (1994). Nerve
768 growth factor contributes to the generation of inflammatory sensory hypersensitivity.
769 *Neuroscience* 62, 327–331. 10.1016/0306-4522(94)90366-2.

770 67. Reis, C., Chambel, S., Ferreira, A., and Cruz, C.D. (2022). Involvement of nerve growth
771 factor (NGF) in chronic neuropathic pain - a systematic review. *Rev Neurosci* 0.
772 10.1515/REVNEURO-2022-0037.

773 68. Bischoff, S., and Dahinden, C. (1992). Effect of Nerve Growth Factor on the Release of
774 Inflammatory Mediators by Mature Human Basophils. *Blood* 79, 2662–2669.
775 10.1182/BLOOD.V79.10.2662.2662.

776 69. Tal, M., and Liberman, R. (1997). Local injection of nerve growth factor (NGF) triggers
777 degranulation of mast cells in rat paw. *Neurosci Lett* 221, 129–132. 10.1016/S0304-
778 3940(96)13318-8.

779 70. Susaki, Y., Shimizu, S., Katakura, K., Watanabe, N., Kawamoto, K., Matsumoto, M.,
780 Tsudzuki, M., Furusaka, T., Kitamura, Y., and Matsuda, H. (1996). Functional Properties
781 of Murine Macrophages Promoted by Nerve Growth Factor. *Blood* 88, 4630–4637.
782 10.1182/BLOOD.V88.12.4630.BLOODJOURNAL88124630.

783 71. Lindholm, D., Heumann, R., Meyer, M., and Thoenen, H. (1987). Interleukin-1 regulates
784 synthesis of nerve growth factor in non-neuronal cells of rat sciatic nerve. *Nature* 330,
785 658–659. 10.1038/330658A0.

786 72. Guerios, S.D., Wang, Z.Y., and Bjorling, D.E. (2006). Nerve growth factor mediates
787 peripheral mechanical hypersensitivity that accompanies experimental cystitis in mice.
788 *Neurosci Lett* 392, 193–197. 10.1016/J.NEULET.2005.09.026.

789 73. Hu, V.Y., Zvara, P., Dattilio, A., Redman, T.L., Allen, S.J., Dawbarn, D., Stroemer, R.P.,
790 and Vizzard, M.A. (2005). Decrease in bladder overactivity with REN1820 in rats with
791 cyclophosphamide induced cystitis. *J Urol* 173, 1016–1021.
792 10.1097/01.JU.0000155170.15023.E5.

793 74. Lane, N.E., Schnitzer, T.J., Birbara, C.A., Mokhtarani, M., Shelton, D.L., Smith, M.D.,
794 and Brown, M.T. (2010). Tanezumab for the treatment of pain from osteoarthritis of the
795 knee. *N Engl J Med* 363, 1521–1531. 10.1056/NEJMoa0901510.

796 75. Brown, M.T., Murphy, F.T., Radin, D.M., Davignon, I., Smith, M.D., and West, C.R.
797 (2012). Tanezumab reduces osteoarthritic knee pain: results of a randomized, double-
798 blind, placebo-controlled phase III trial. *J Pain* 13, 790–798.
799 10.1016/J.JPAIN.2012.05.006.

800 76. Spierings, E.L.H., Fidelholtz, J., Wolfram, G., Smith, M.D., Brown, M.T., and West, C.R.
801 (2013). A phase III placebo- and oxycodone-controlled study of tanezumab in adults with
802 osteoarthritis pain of the hip or knee. *Pain* 154, 1603–1612. 10.1016/J.PAIN.2013.04.035.

803 77. Balanescu, A.R., Feist, E., Wolfram, G., Davignon, I., Smith, M.D., Brown, M.T., and
804 West, C.R. (2014). Efficacy and safety of tanezumab added on to diclofenac sustained
805 release in patients with knee or hip osteoarthritis: a double-blind, placebo-controlled,
806 parallel-group, multicentre phase III randomised clinical trial. *Ann Rheum Dis* 73, 1665–
807 1672. 10.1136/ANRHEUMDIS-2012-203164.

808 78. Katz, N., Borenstein, D.G., Birbara, C., Bramson, C., Nemeth, M.A., Smith, M.D., and
809 Brown, M.T. (2011). Efficacy and safety of tanezumab in the treatment of chronic low
810 back pain. *Pain* 152, 2248–2258. 10.1016/J.PAIN.2011.05.003.

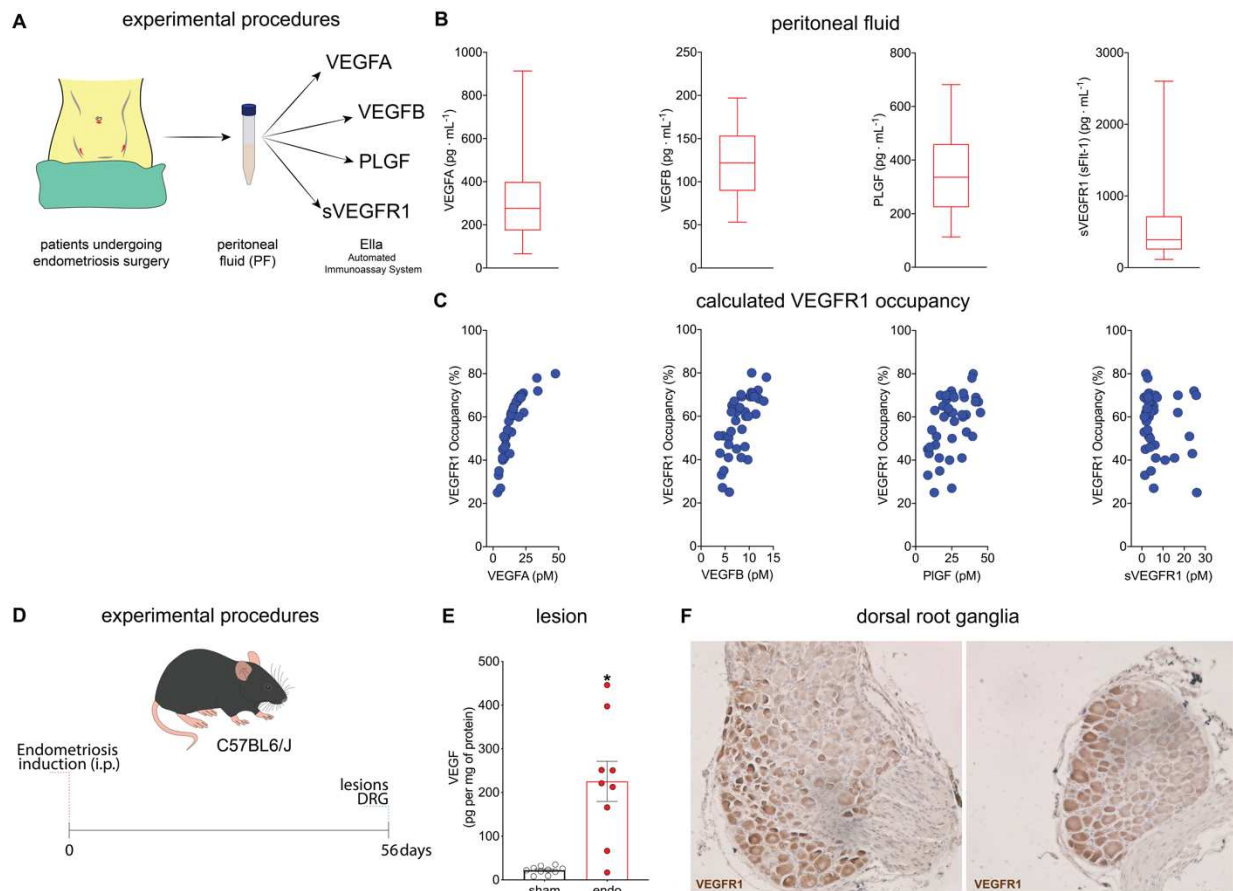
811 79. Bramson, C., Herrmann, D., Biton, V., Carey, W., Keller, D., Brown, M., West, C.,
812 Verburg, K., and Dyck, P. (2013). Efficacy and safety of subcutaneous tanezumab in
813 patients with pain related to diabetic peripheral neuropathy (NCT01087203). *J Pain* *14*,
814 S68. 10.1016/j.jpain.2013.01.610.

815 80. Evans, R.J., Moldwin, R.M., Cossons, N., Darekar, A., Mills, I.W., and Scholfield, D.
816 (2011). Proof of concept trial of tanezumab for the treatment of symptoms associated with
817 interstitial cystitis. *J Urol* *185*, 1716–1721. 10.1016/J.JURO.2010.12.088.

818

819

820 **Figures**



821

822 **Figure 1. Levels of VEGFR1 ligands are increased in the peritoneal fluid of endometriosis**
823 **patients and in mouse lesions.** (A) experimental procedures for peritoneal fluid collection of

824 endometriosis patients. (B) The levels of VEGFA, VEGFB, PI GF, and sVEGFR1 in peritoneal

825 fluid samples determined by Ella®. Data are presented in box and whisker charts representing the

826 levels of each mediator in pg/mL. (C) Calculated VEGFR1 occupancy. Note that in published data,

827 occupancy is approximately proportional to signalling⁶⁵. (D) Experimental procedures and

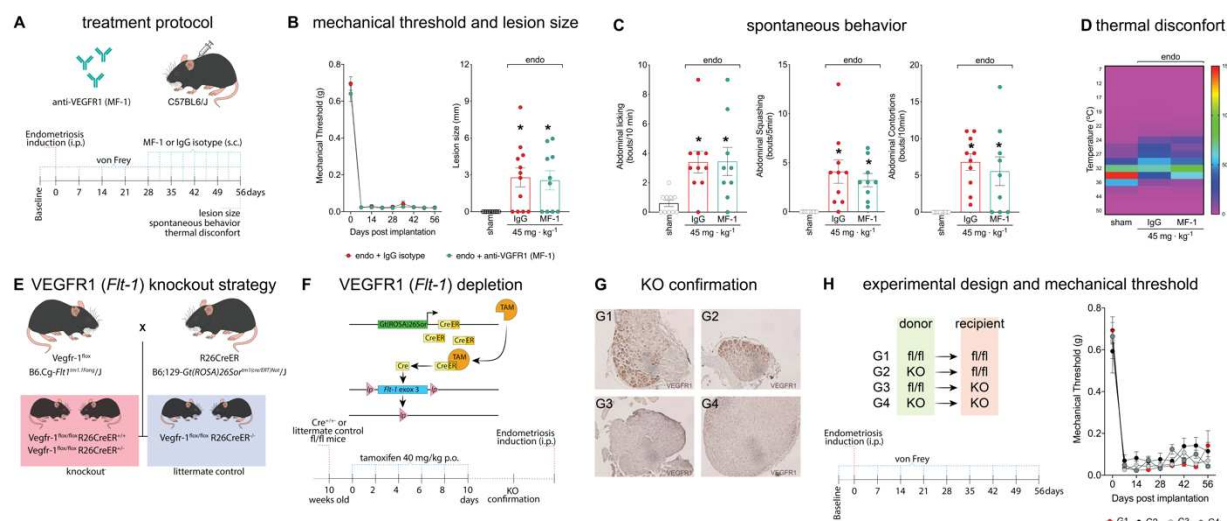
828 timepoints for tissue collection in our mouse model. (E) 56 days after endometriosis induction,

829 mouse lesions were collected for determination of VEGF levels by ELISA. Results are presented

830 as mean ± SEM of VEGF levels, n = 10 (sham – uterine horn tissue), and n = 9 (endo) mice per

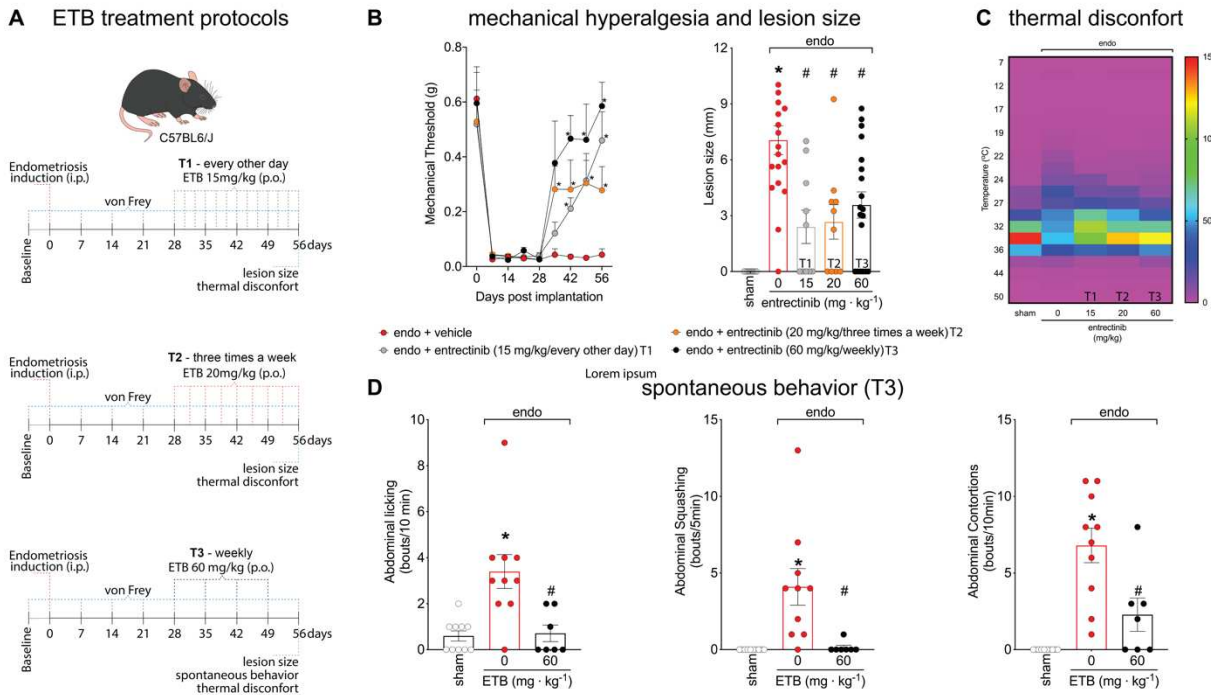
831 group (*P < 0.05 vs. sham). (F) expression profile of VEGFR1 expression in DRG nociceptors

832 determined by immunohistochemistry 56 days after endometriosis induction.



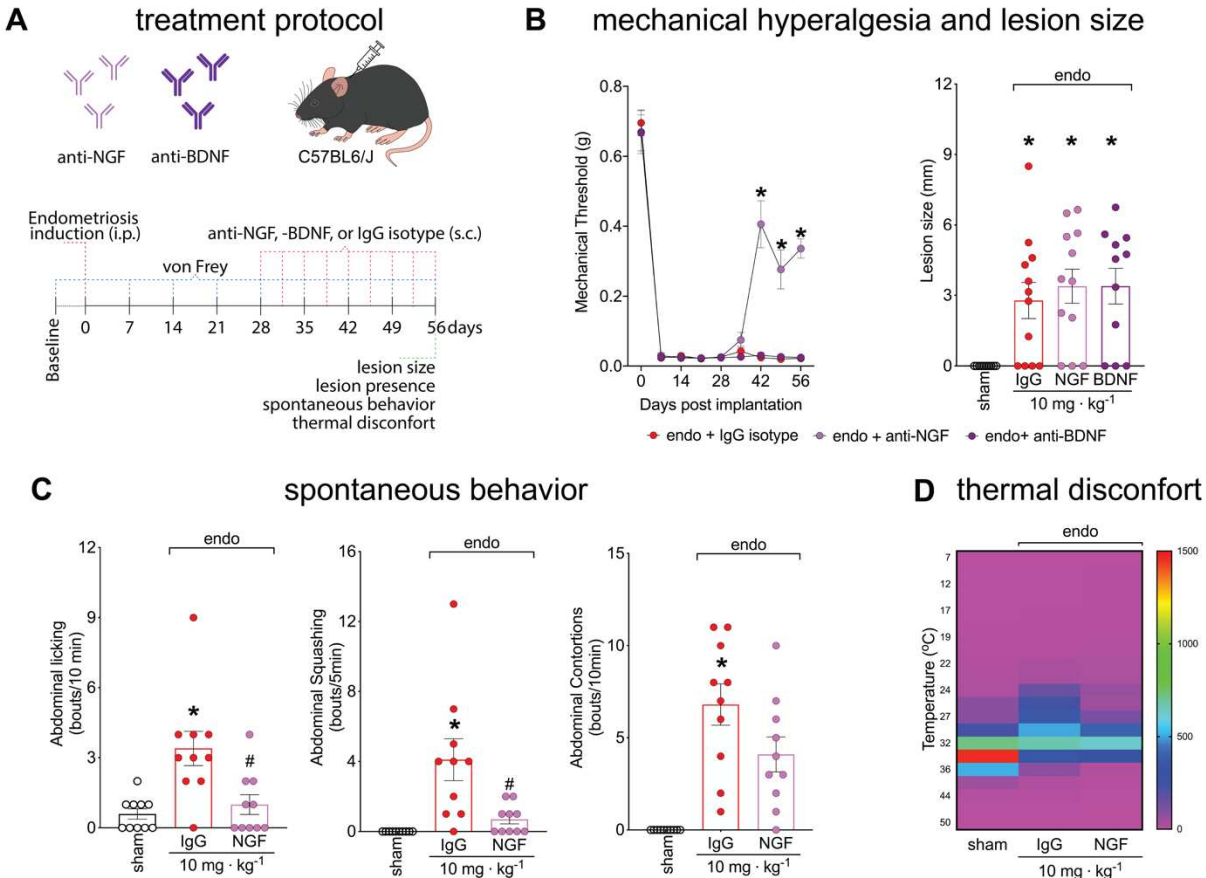
833

834 **Figure 2. VEGF neutralization or VEGFR1 ablation do not reduce endometriosis-associated**
 835 **pain or thermal discomfort in mice.** (A) scheme of the treatment protocol with anti-VEGFR1
 836 (MF-1) antibody and IgG control. (B) mechanical hyperalgesia was determined using von Frey
 837 filaments before (zero) and after (7, 14, 21, 28, 35, 42, and 56 days) endometriosis induction.
 838 Results are presented as mean \pm SEM of mechanical threshold, n = 10 mice per group. (C)
 839 spontaneous behaviours measurements. For abdominal licking, the total number of times that mice
 840 directly groomed the abdominal region (without going to any other body region before or after the
 841 behaviour) was quantified for 10 minutes. For abdominal squashing, the number of times the mice
 842 pressed the lower abdominal region against the floor was quantified for 5 minutes. Sham mice did
 843 not display abdominal squashing. Abdominal contortions were quantified for 10 minutes by
 844 counting the number of contractions of the abdominal muscle together with stretching of hind
 845 limbs. Sham mice did not display abdominal contortions. Results are expressed as mean \pm SEM of
 846 abdominal licking, squashing, and contortions bouts per minute, n = 9-12. (*P < 0.05 vs. sham).
 847 (D) thermal discomfort heatmap. Heatmap shows mean time spent in each temperature zone for
 848 IgG control- or MF-1-treated mice. Data are presented as mean \pm SEM of the amplitude of
 849 permanence in seconds in each thermal zone during 60 min, n = 9-12. (E) breeding scheme for
 850 generation of VEGFR1 tamoxifen-induced cre-dependent knockout strategy. (F) scheme of
 851 tamoxifen-induced cre-dependent VEGFR1 knockout and tamoxifen treatment protocol. (G) DRG
 852 neuron representative images for VEGFR1 knockout confirmation determined per IHC analysis.
 853 G1-G2 from littermate controls and G3-G4 from knockout mice n = 10. (H) Endometriosis
 854 induction protocol scheme with receptor and donor combinations. Mechanical response before
 855 (zero) and after (7, 14, 21, 28, 35, 42, and 56 days) endometriosis induction using von Frey
 856 filaments. Results are presented as mean \pm SEM of mechanical threshold, n = 10 mice per group.



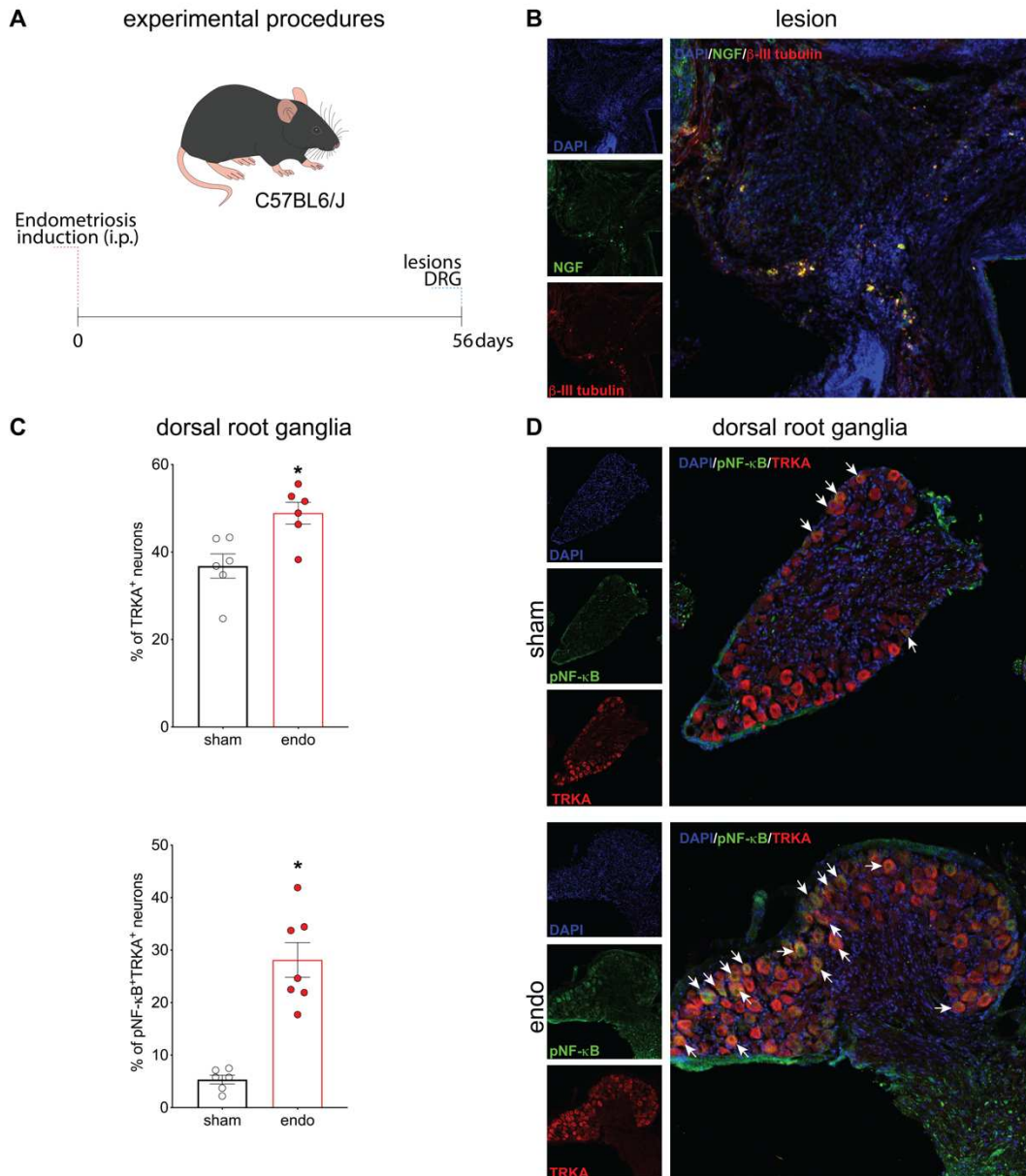
857

858 **Figure 3. Entrectinib, a pan-Trk inhibitor, reduces endometriosis-associated pain and**
 859 **thermal discomfort.** (A) scheme of the treatment protocol with entrectinib. T1: 15 mg/kg every
 860 other day; T2: 20 mg/kg three times a week; and T3: 60 mg/kg weekly. In all schedules of
 861 treatment, the maximum weekly dose is 60 mg/kg. (B left) mechanical response before (zero) and
 862 after (7, 14, 21, 28, 35, 42, and 56 days) endometriosis induction using von Frey filaments. Results
 863 are presented as mean \pm SEM of mechanical threshold, $n = 10$ mice per group (* $P < 0.05$ vs.
 864 vehicle-treated group). (B right) lesion size. Results are presented as mean \pm SEM of lesion size
 865 in mm, $n = 10-19$ mice per group (* $P < 0.05$ vs. sham, # $P < 0.05$ vs. vehicle-treated group). (C)
 866 thermal discomfort heatmap. Data are presented as mean \pm SEM of the amplitude of permanence
 867 in seconds in each thermal zone during 60 min. (D) spontaneous behaviour measurements. For
 868 abdominal licking, the total number of times that mice directly groomed the abdominal region
 869 (without going to any other body region before or after the behaviour) was quantified for 10
 870 minutes. For abdominal squashing, the number of times the mice pressed the lower abdominal
 871 region against the floor was quantified for 5 minutes. Sham mice did not display abdominal
 872 squashing. Abdominal contortions were quantified for 10 minutes by counting the number of
 873 contractions of the abdominal muscle together with stretching of hind limbs. Sham mice did not
 874 display abdominal contortions. Results are expressed as mean \pm SEM of abdominal licking,
 875 squashing, and contortions bouts per minute, $n = 7-10$. (* $P < 0.05$ vs. sham, # $P < 0.05$ vs. vehicle-
 876 treated group).



877

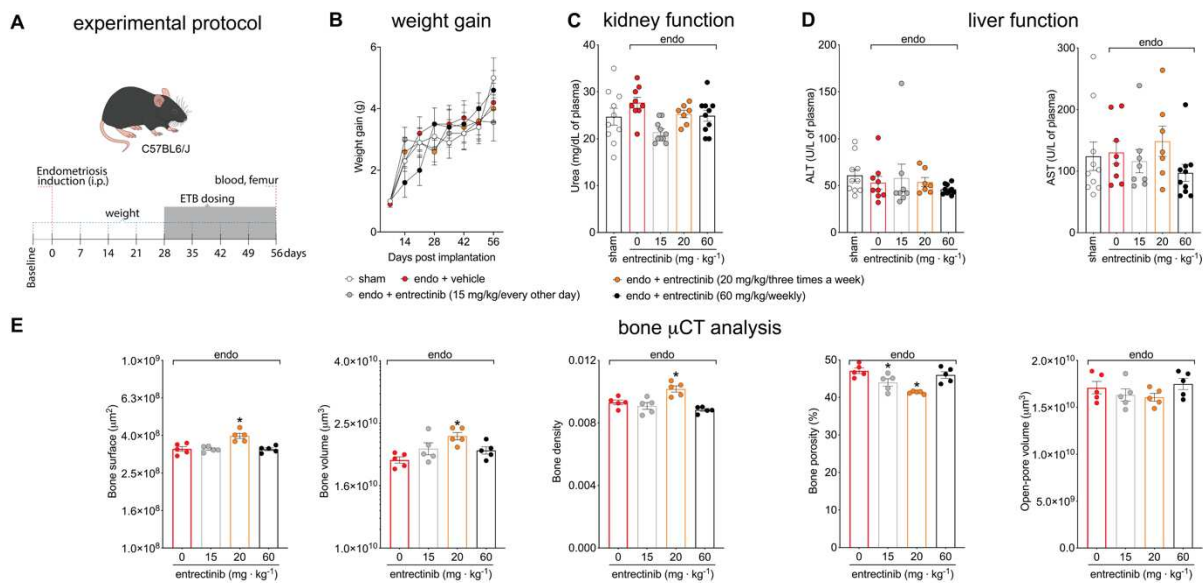
878 **Figure 4. NGF, but not BDNF neutralization, reduces endometriosis-associated pain and**
 879 **thermal discomfort in mice.** (A) scheme of the treatment protocol with IgG control, anti-NGF,
 880 or anti-BDNF antibodies. (B) mechanical hyperalgesia was measured using von Frey filaments
 881 before (zero) and after (7, 14, 21, 28, 35, 42, and 56 days) endometriosis induction. Results are
 882 presented as mean \pm SEM of mechanical threshold, $n = 10-12$ mice per group (* $P < 0.05$ vs. IgG
 883 treated group). (C) spontaneous behaviours measurements. For abdominal licking, the total
 884 number of times that mice directly groomed the abdominal region (without going to any other
 885 body region before or after the behaviour) was quantified for 10 minutes. For abdominal
 886 squashing, the number of times the mice pressed the lower abdominal region against the floor was
 887 quantified for 5 minutes. Sham mice did not display abdominal squashing. Abdominal contortions
 888 were quantified for 10 minutes by counting the number of contractions of the abdominal muscle
 889 together with stretching of hind limbs. Sham mice did not display abdominal contortions. Results
 890 are expressed as mean \pm SEM of abdominal licking, squashing, and contortions bouts per minute,
 891 $n = 10$ mice per group. (* $P < 0.05$ vs. sham, # $P < 0.05$ vs. IgG control). (D) thermal discomfort
 892 heatmap. Heatmap shows mean time spent in each temperature zone for IgG control-, anti-NGF-,
 893 or anti-BDNF-treated mice. Data are presented as mean \pm SEM of the amplitude of permanence
 894 in seconds in each thermal zone during 60 min, $n = 10$ mice per group.



895

896 **Figure 5. NGF-TrkA signaling is activated during endometriosis.** (A) scheme of experimental
897 procedures. (B) representative image from endometriotic lesions stained for NGF and beta-III
898 tubulin. (C) quantification of TrkA⁺ and pNF-κB⁺TrkA⁺ neurons in dorsal root ganglia (DRG) of
899 sham and endometriosis lesion-bearing mice. Lesions and DRG were dissected at 56 dpi. Results
900 are presented as mean \pm SEM of the percentage of positive neurons. n = 6 or 7 mice per group. (*P
901 < 0.05 vs. sham). (D) Representative images of DRG neurons stained for TrkA (red) and p-NF-κB
902 (green) by confocal microscopy.

903



904

905 **Figure 6. Weekly treatment with entrectinib does not induce weight change, liver or kidney**
906 **toxicity, or bone loss in mice.** (A) scheme of experimental protocol for determination of

907 entrectinib safety using the different treatment schedules. (B) mouse weight was determined

908 weekly. Results are presented as mean \pm SEM in grams, n = 7-10 mice per group. (C) kidney

909 function was determined by measuring urea plasma levels. Results are presented as mean \pm SEM

910 of urea levels, n = 7-10 mice per group. (D) liver function was determined by measuring ALT and

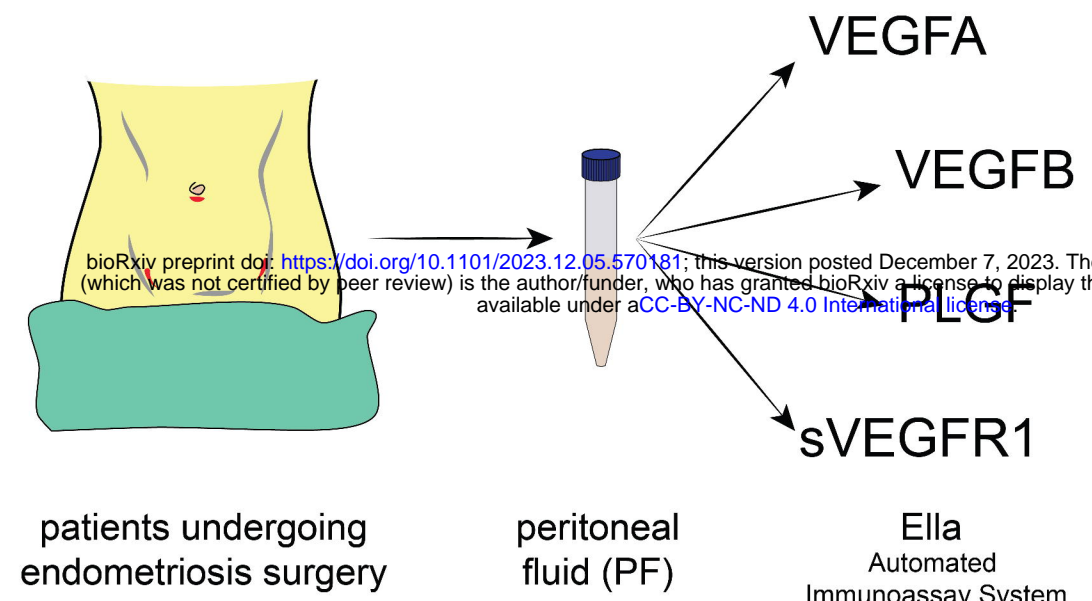
911 AST plasma levels. Blood and femur were collected 56 dpi (after 4 weeks of treatment). Results

912 are presented as mean \pm SEM of AST and ALT levels, n = 7-10 mice per group. (E)

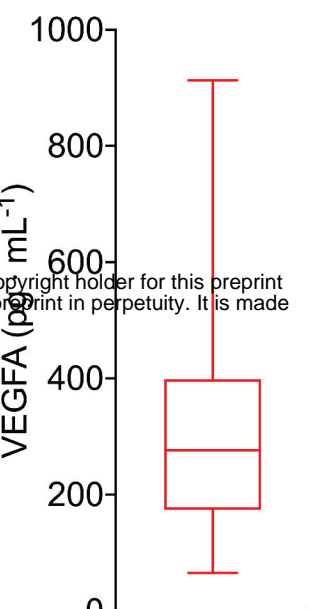
913 Microcomputed tomography of bone (femur) was used to determine bone loss. Results are

914 presented as mean \pm SEM, n = 5 mice per group.

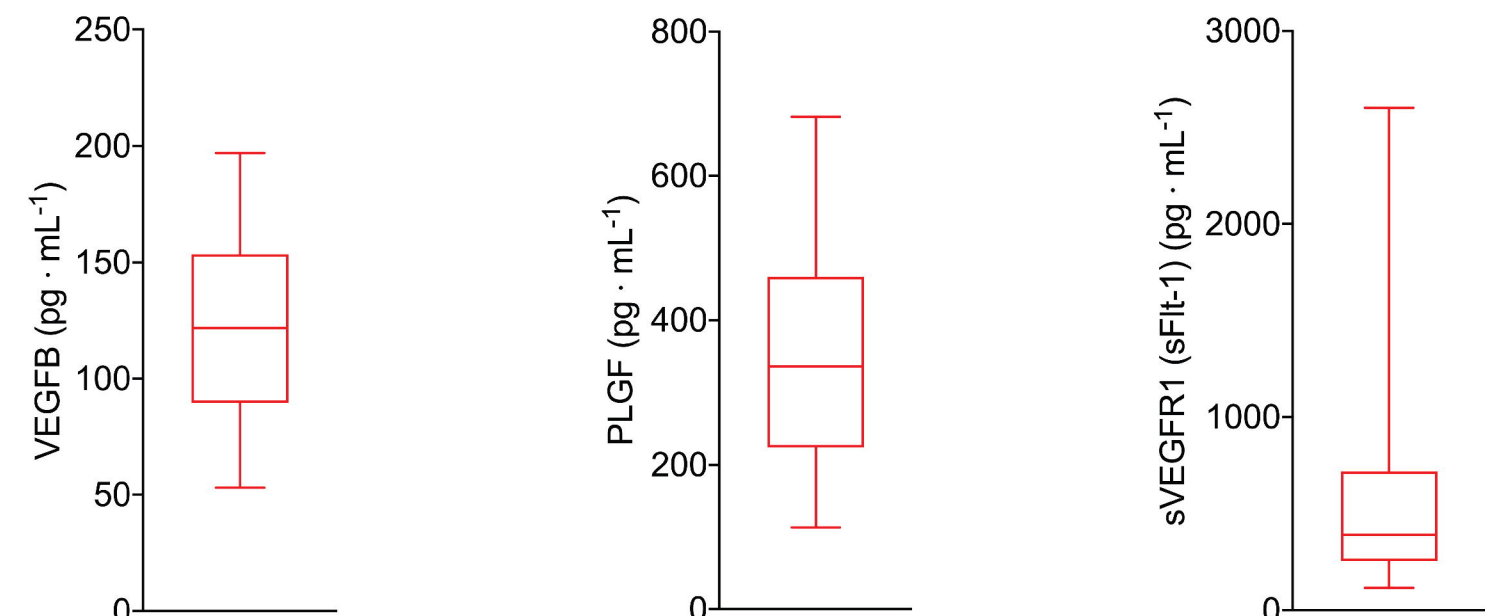
A experimental procedures



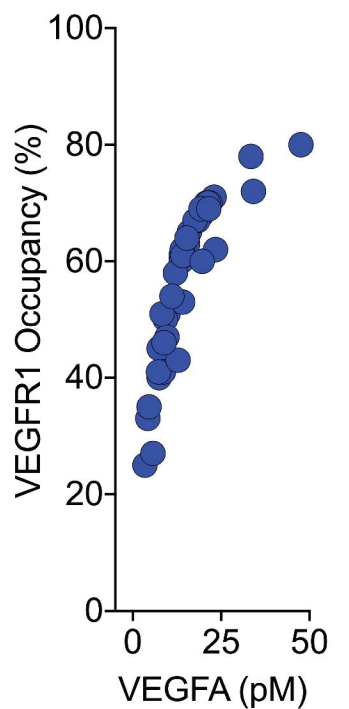
B



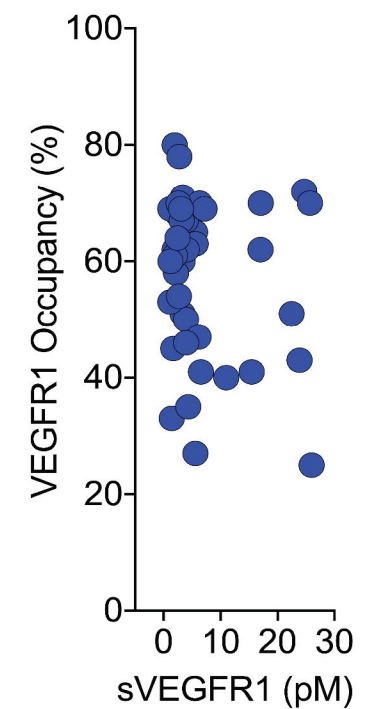
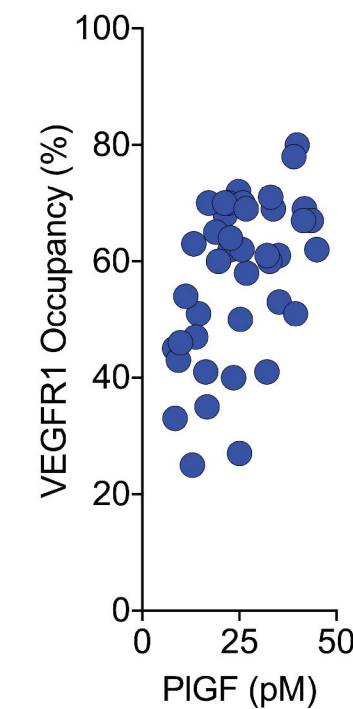
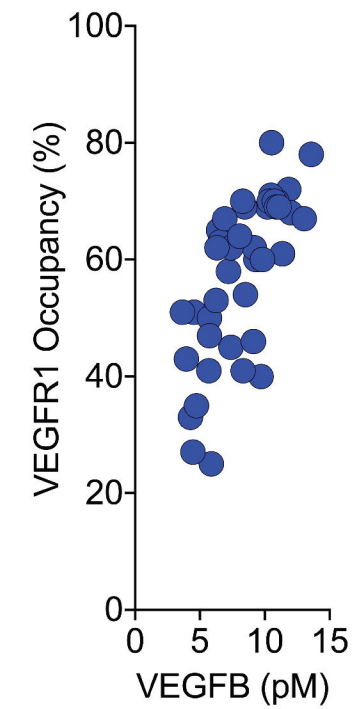
peritoneal fluid



C



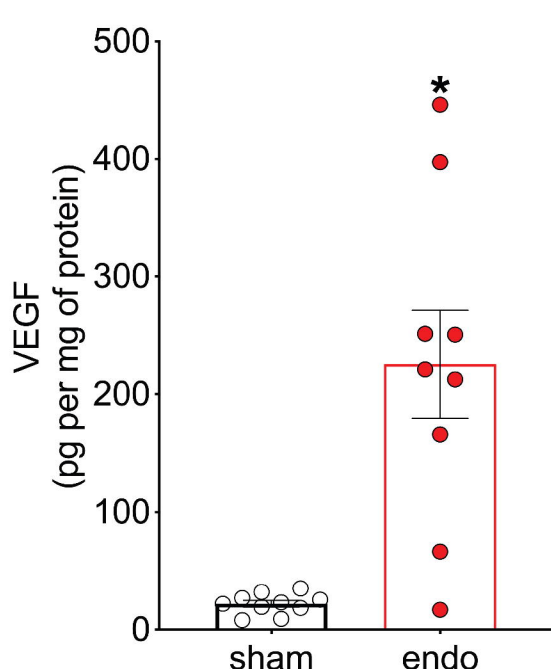
calculated VEGFR1 occupancy



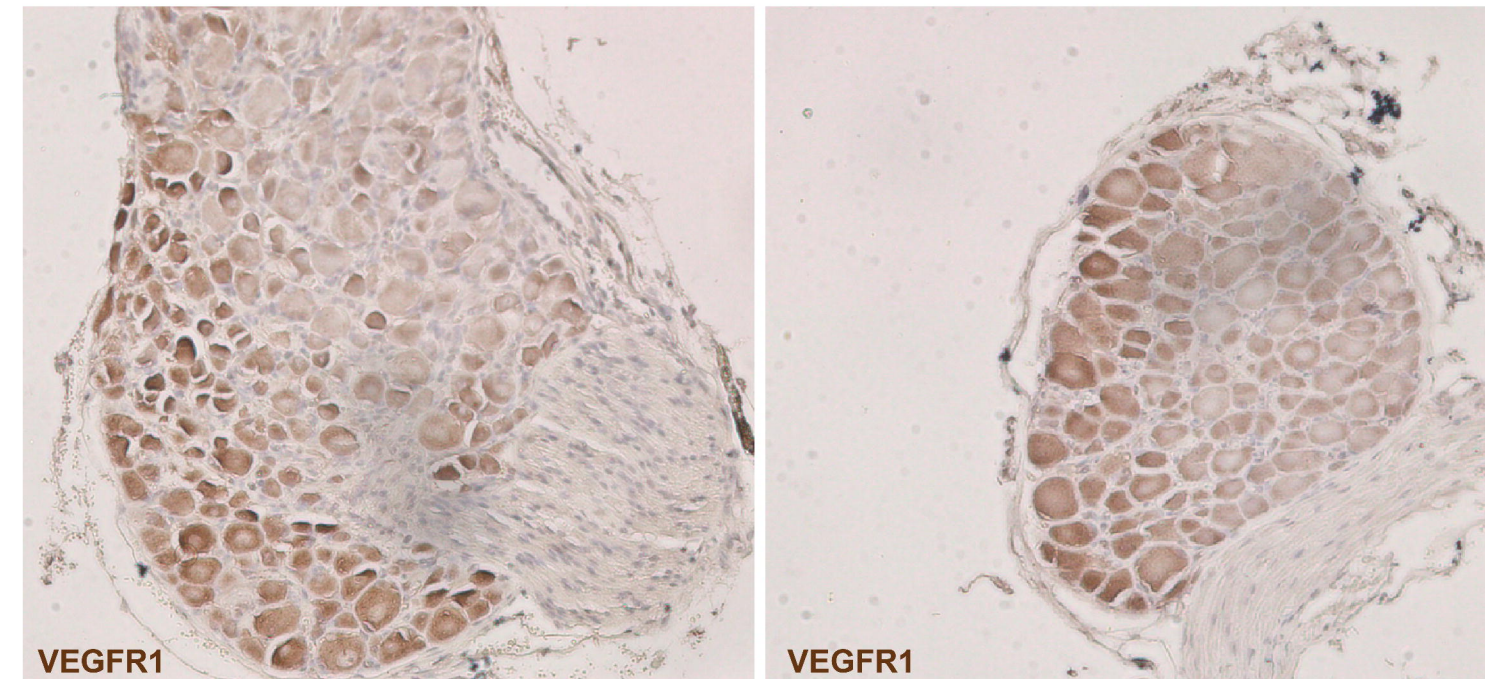
D experimental procedures

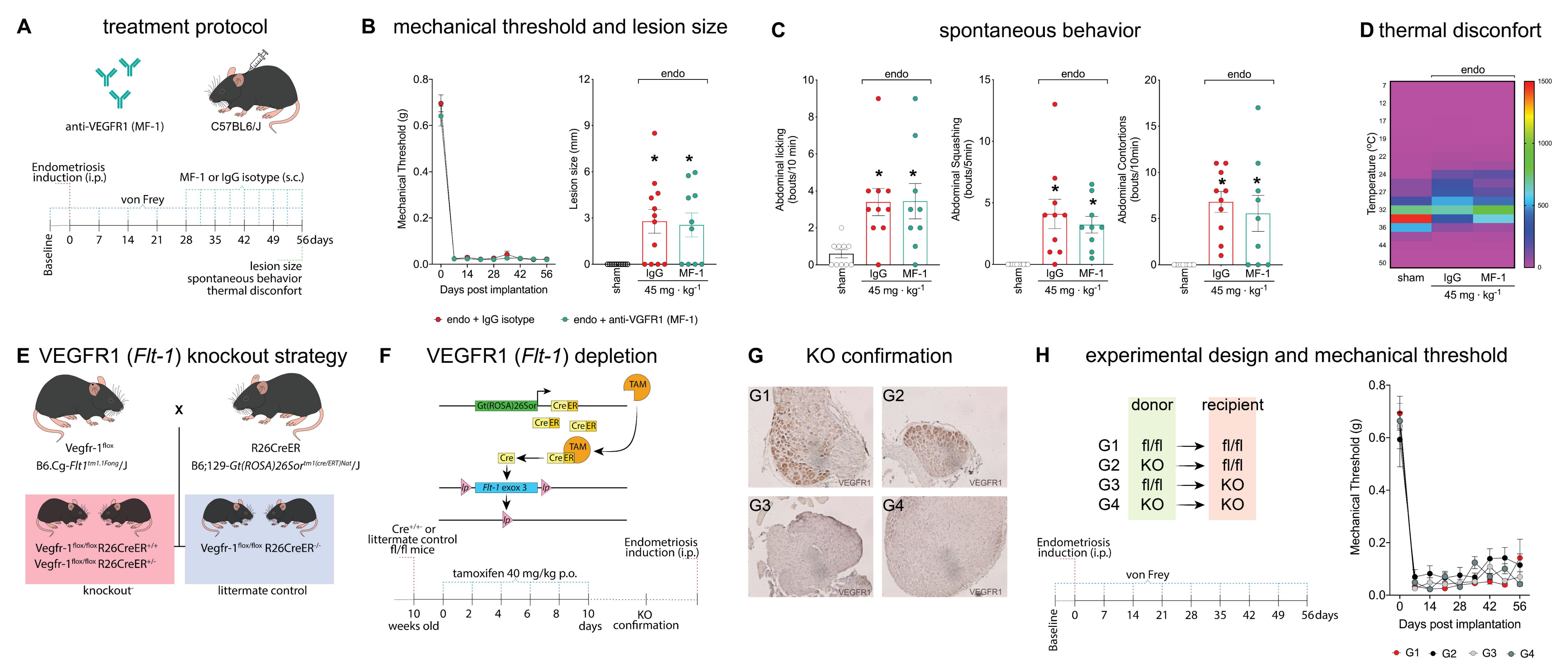


E lesion

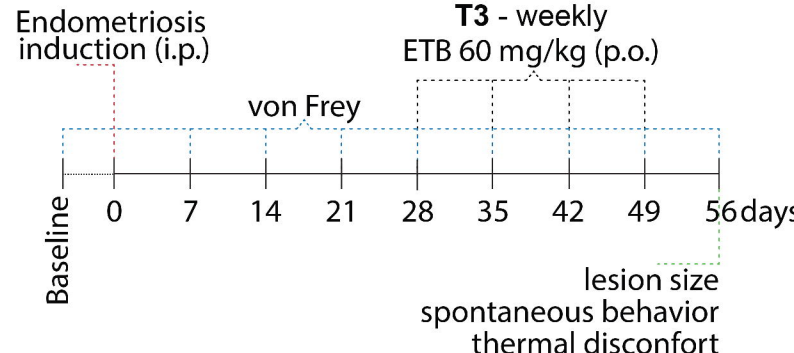
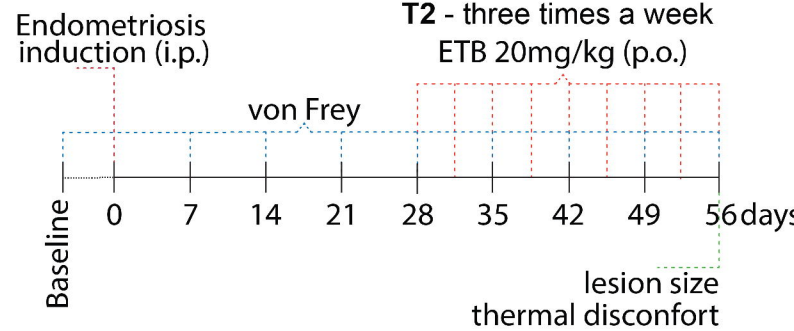
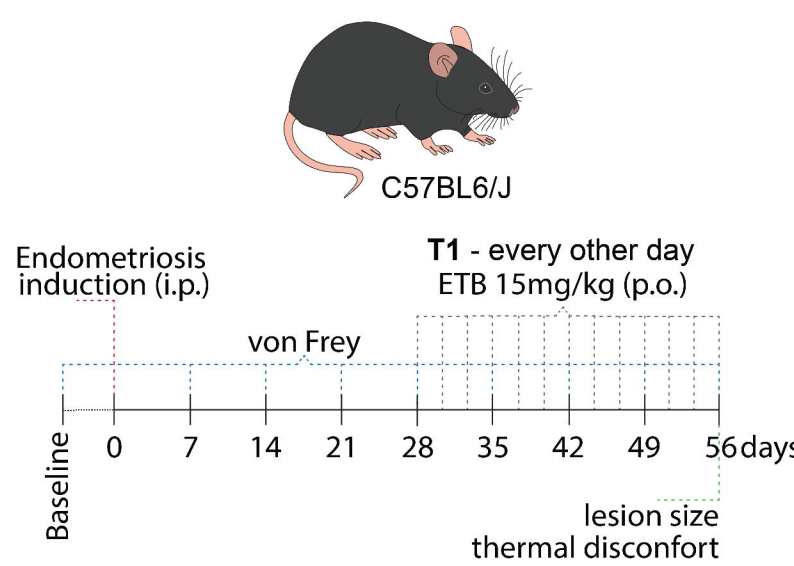


F dorsal root ganglia

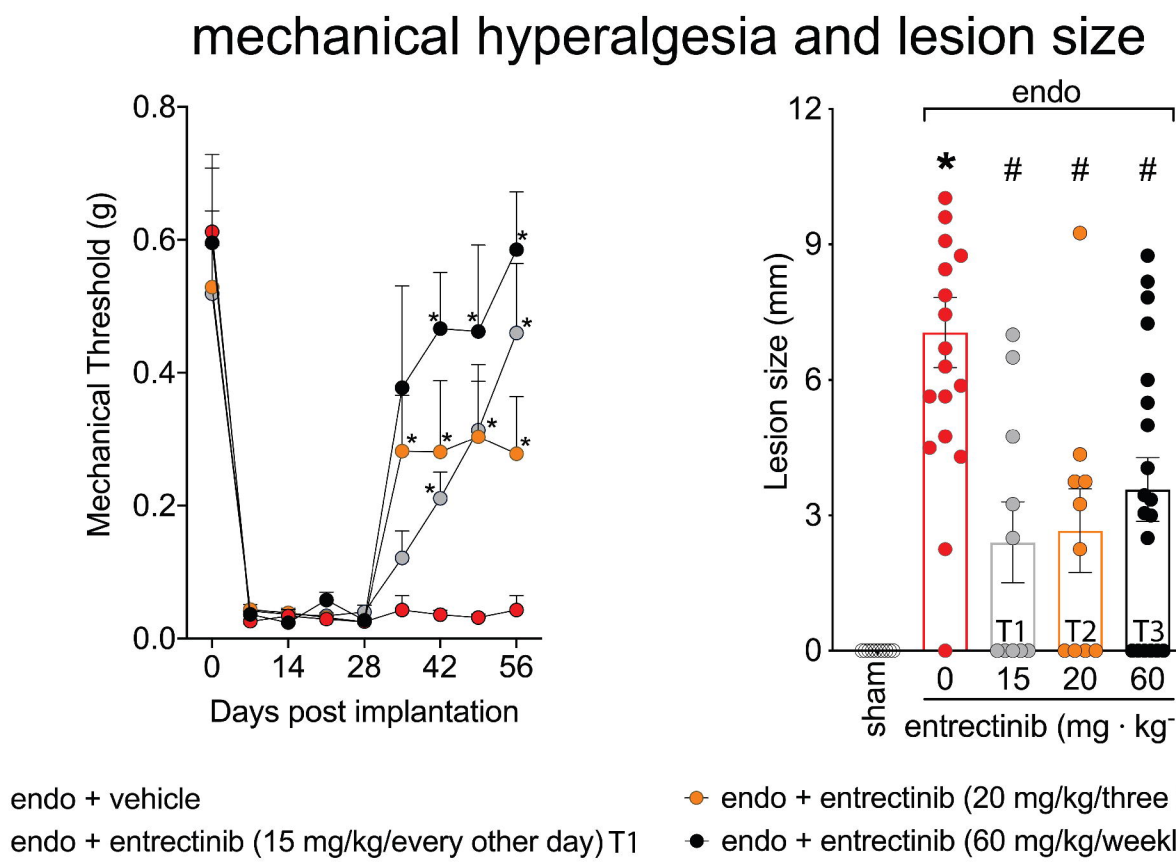




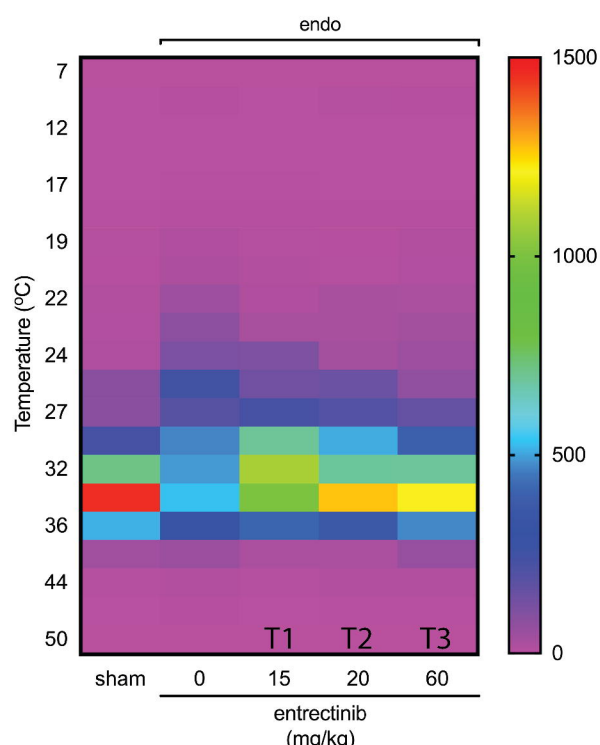
A ETB treatment protocols



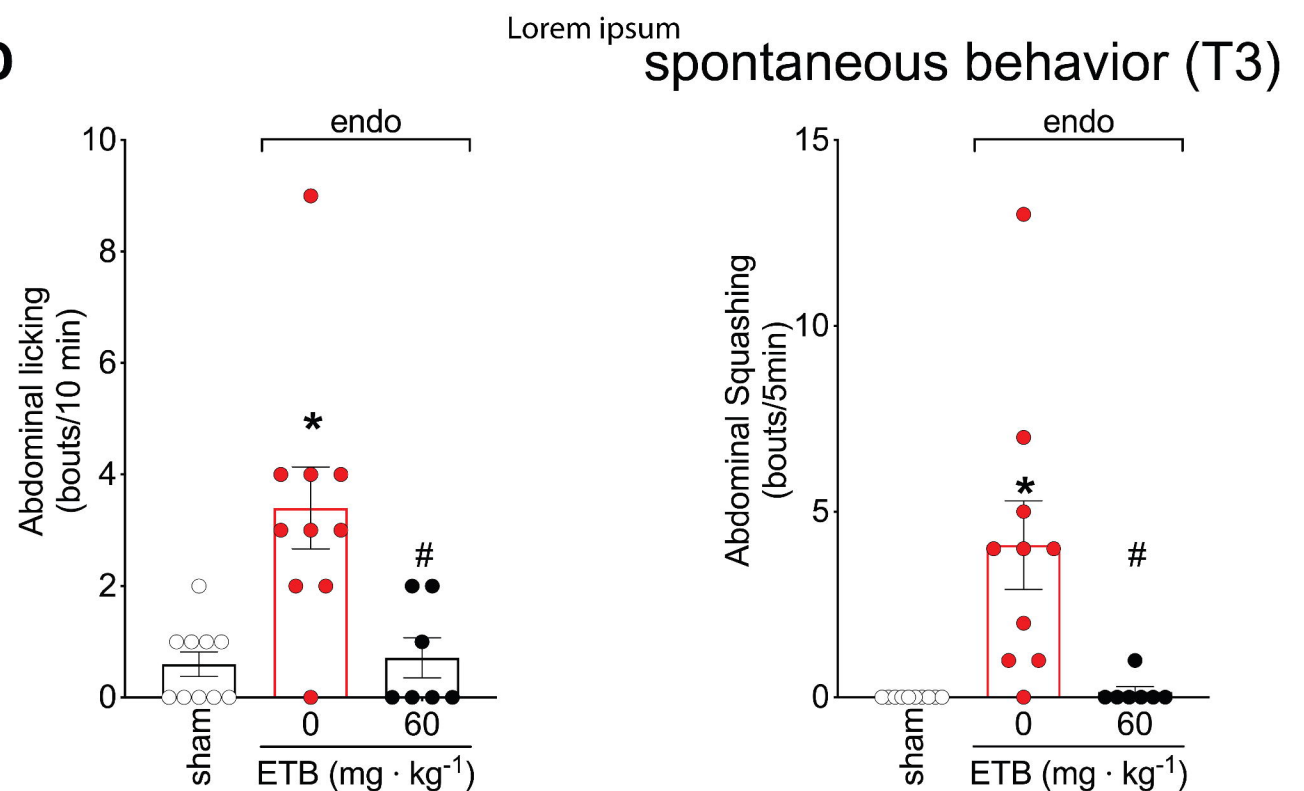
B

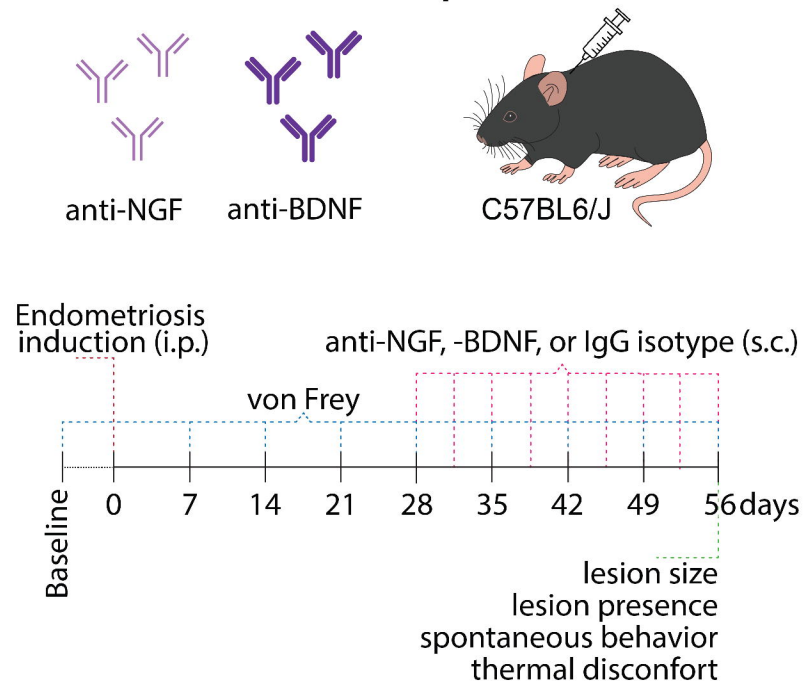
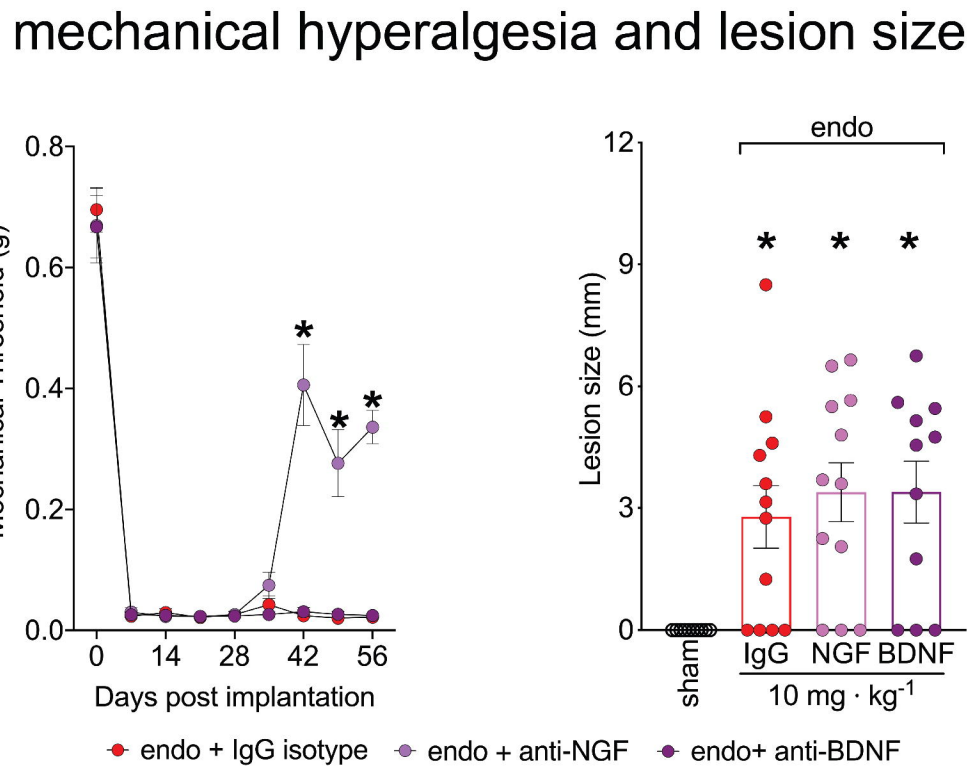
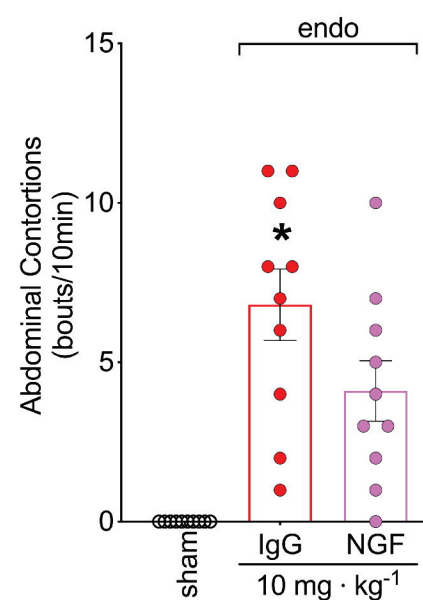
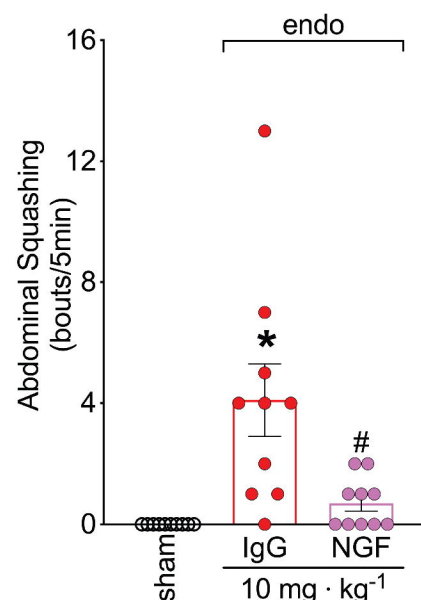
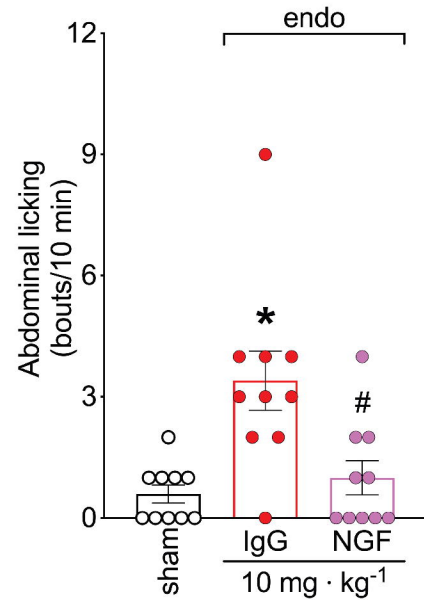
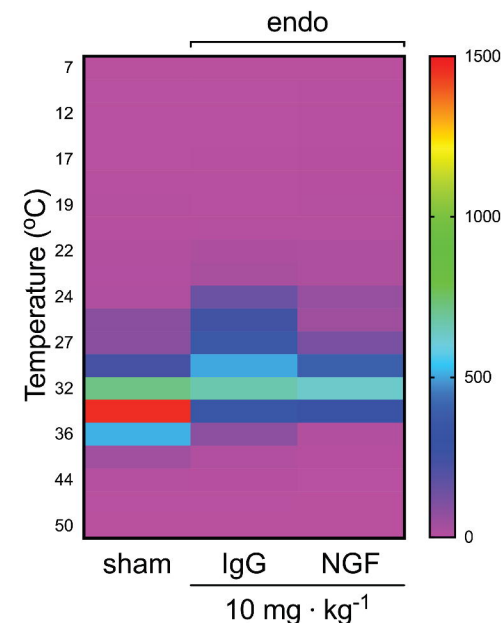


C



D



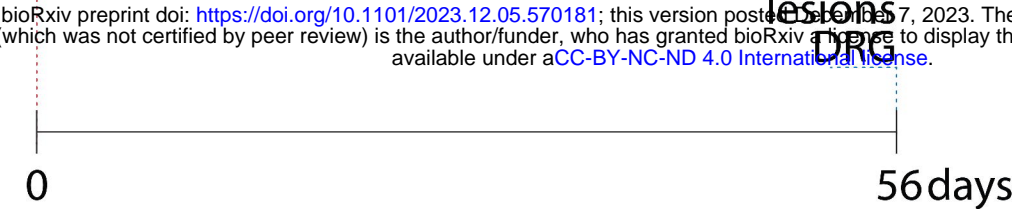
A**treatment protocol****B****C****spontaneous behavior****thermal discomfort**

A experimental procedures

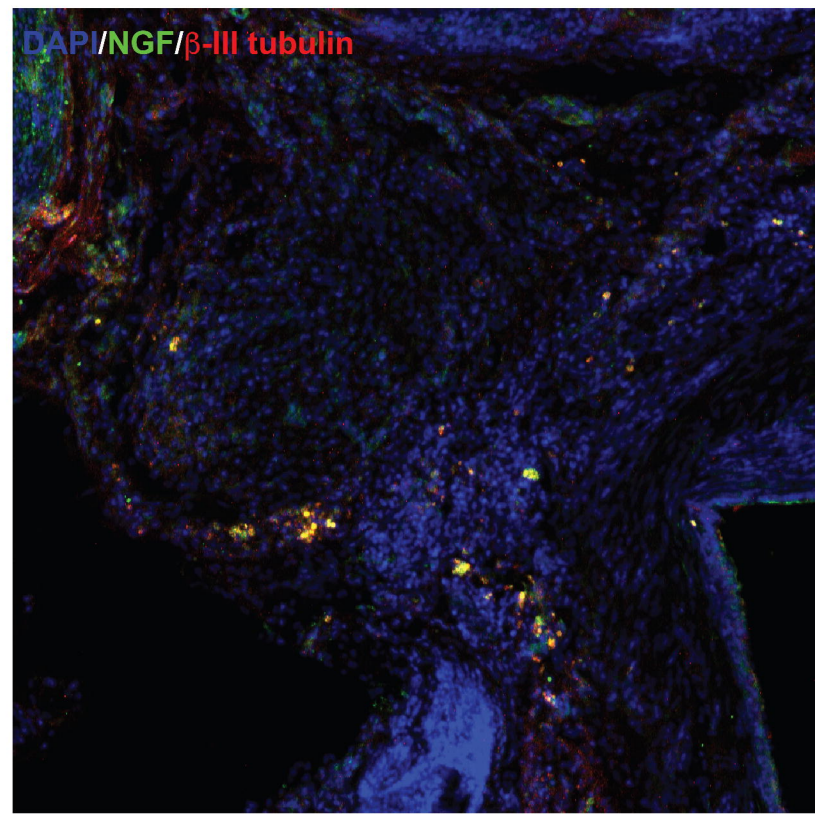
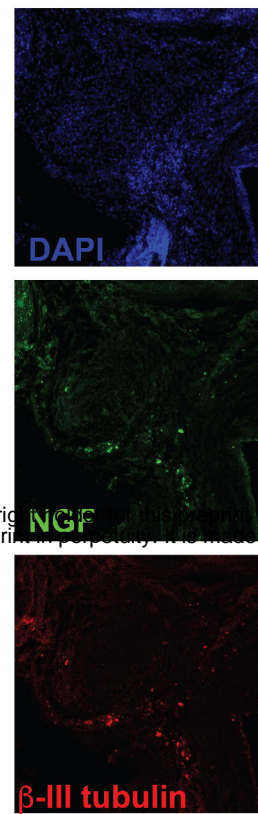


C57BL/6J

Endometriosis induction (i.p.)

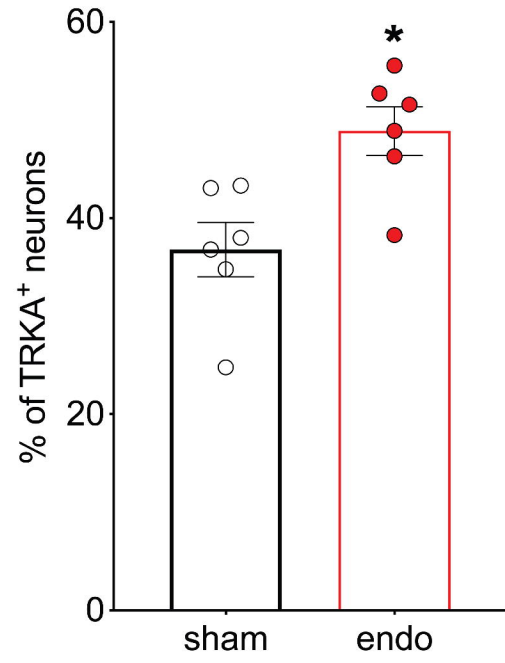


B lesion



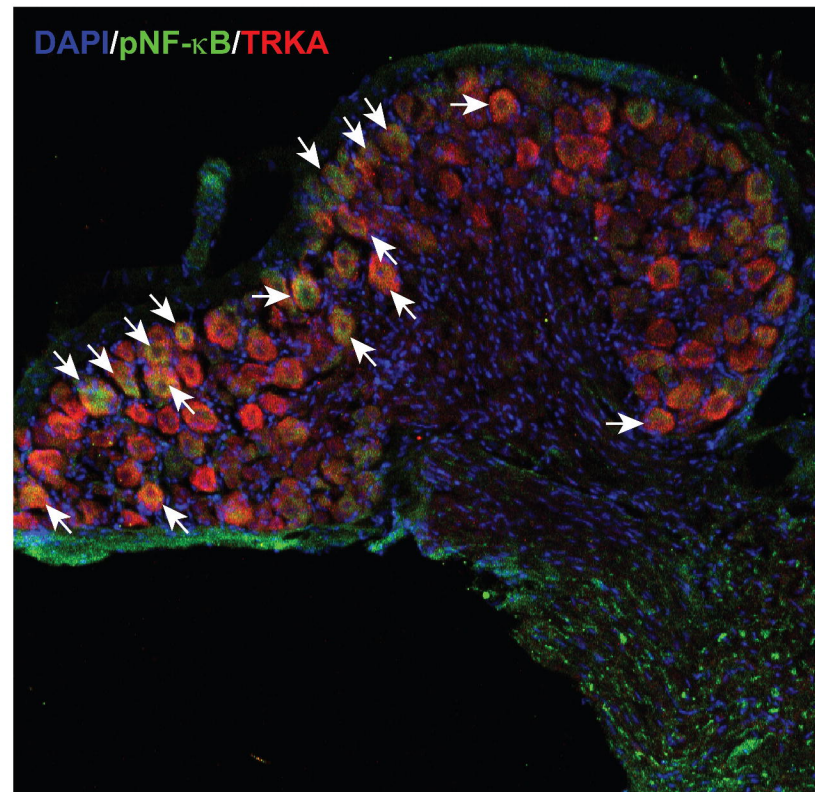
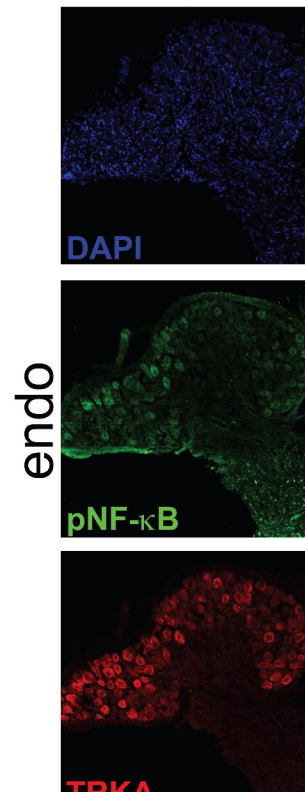
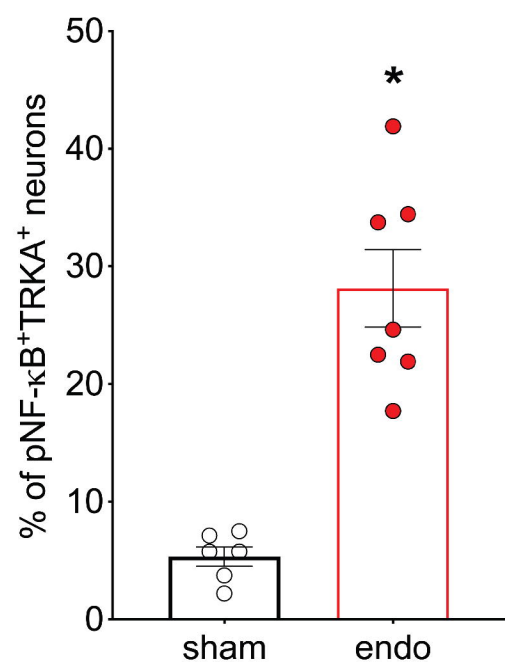
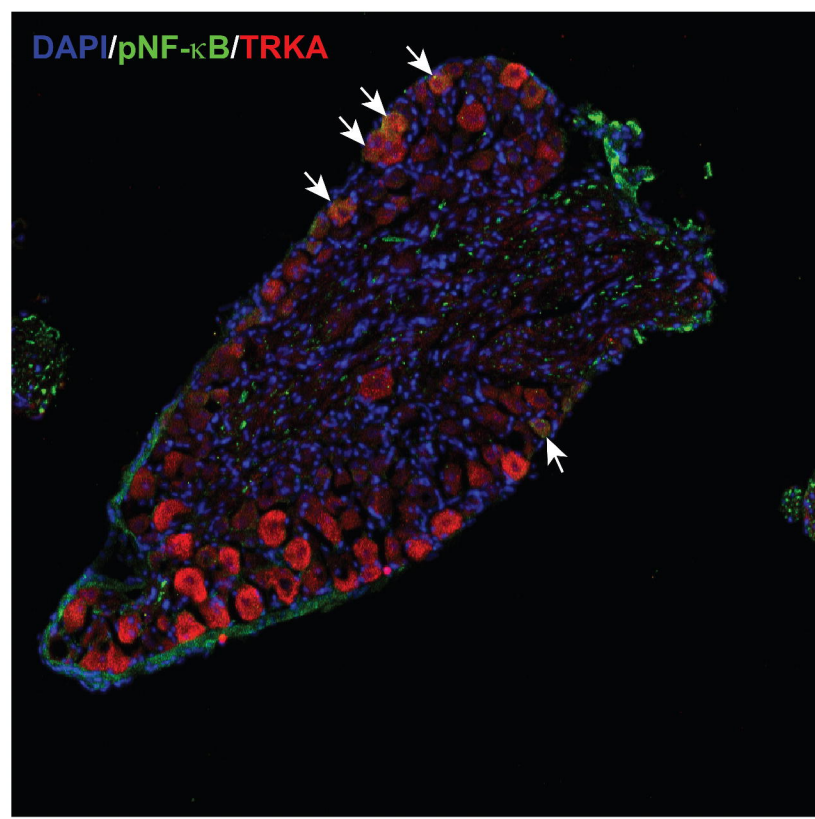
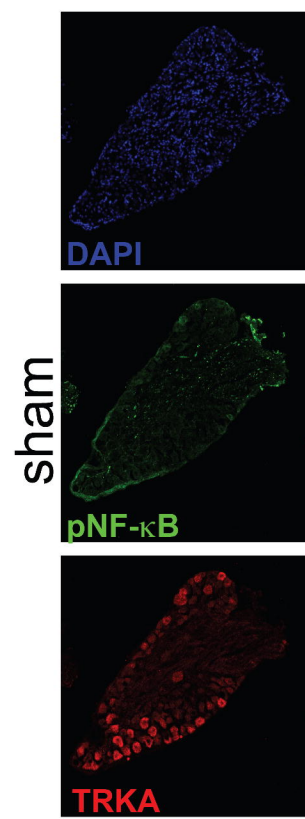
C

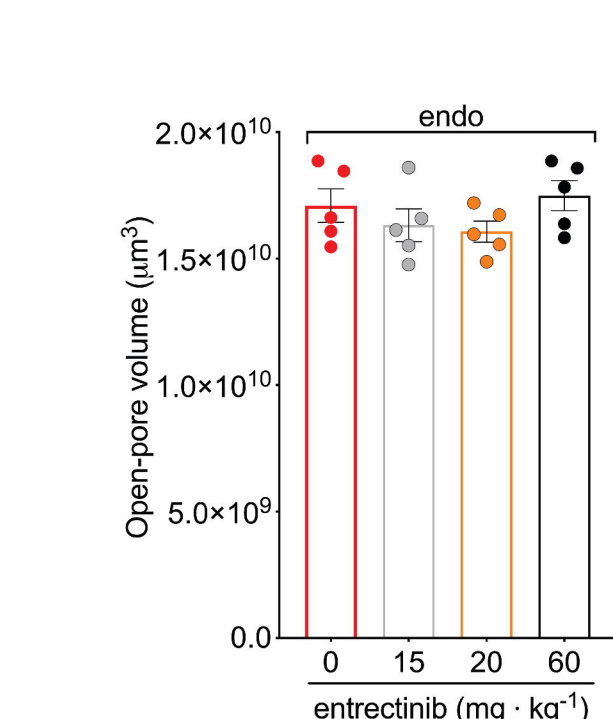
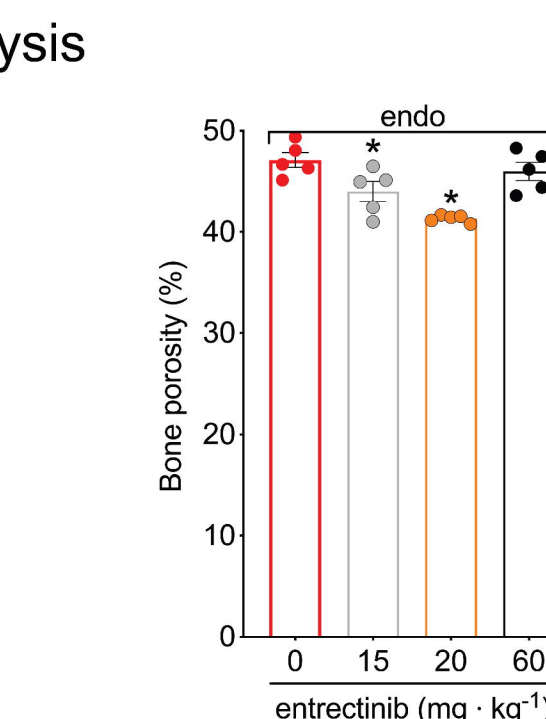
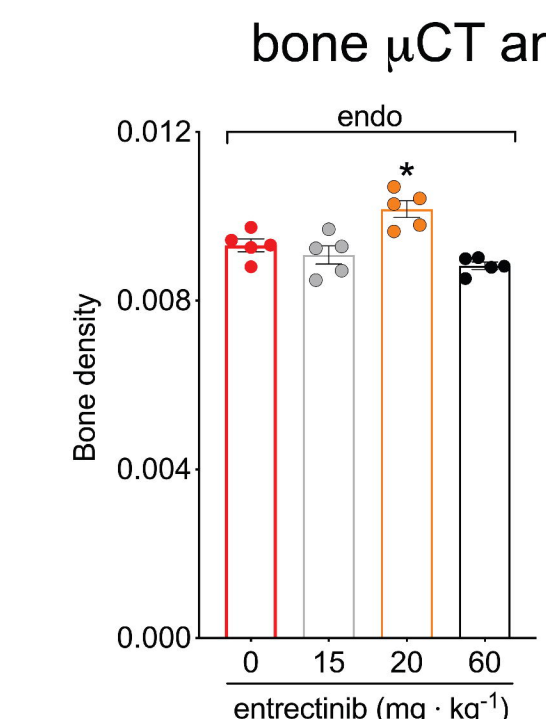
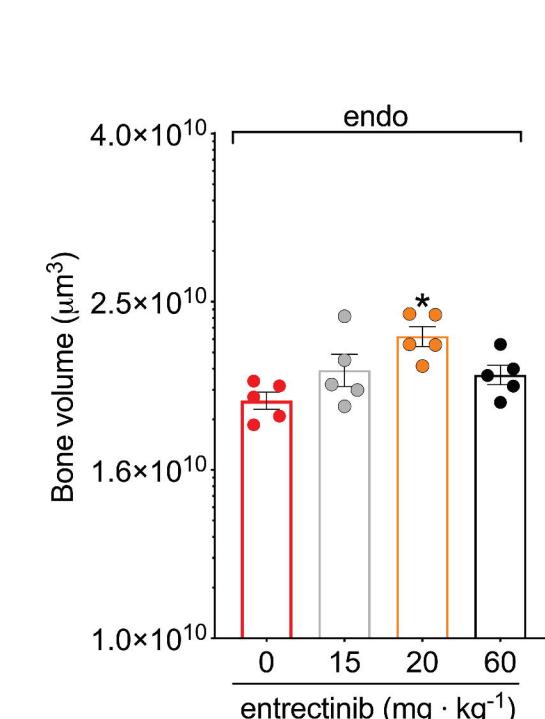
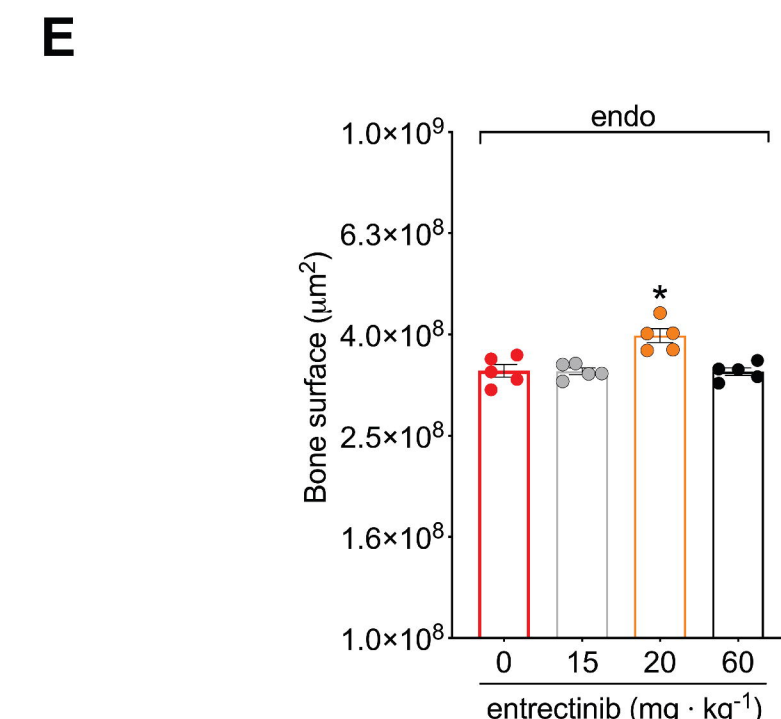
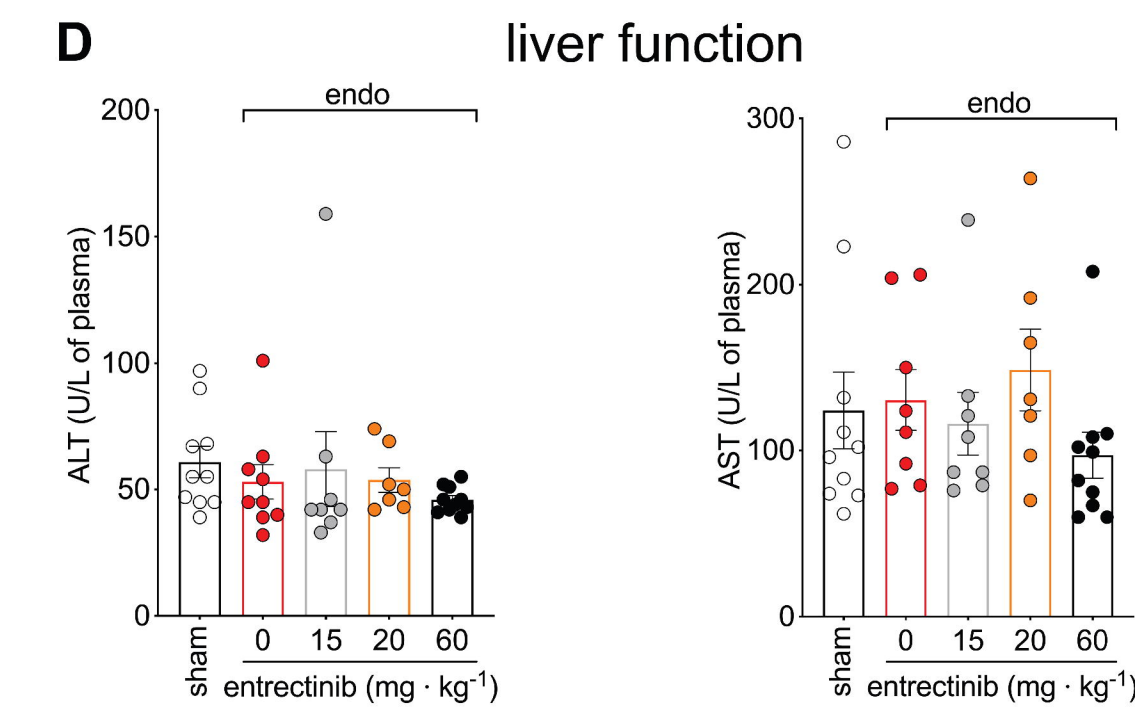
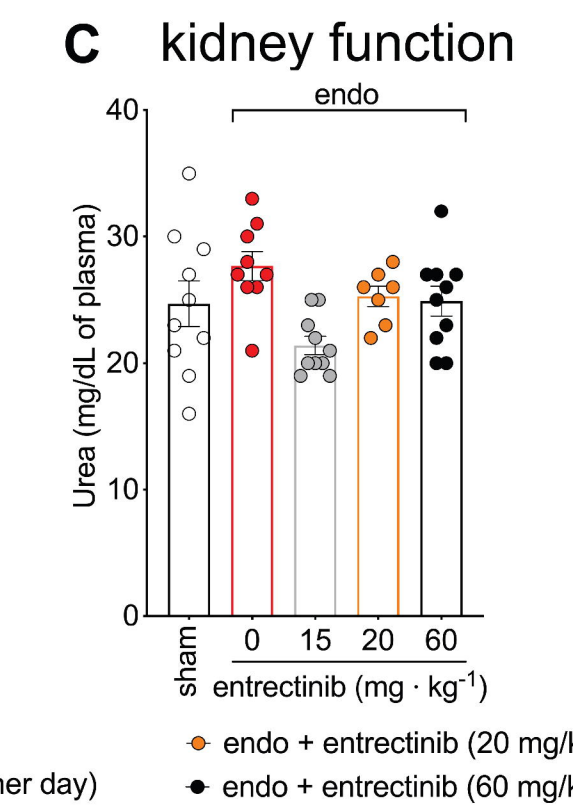
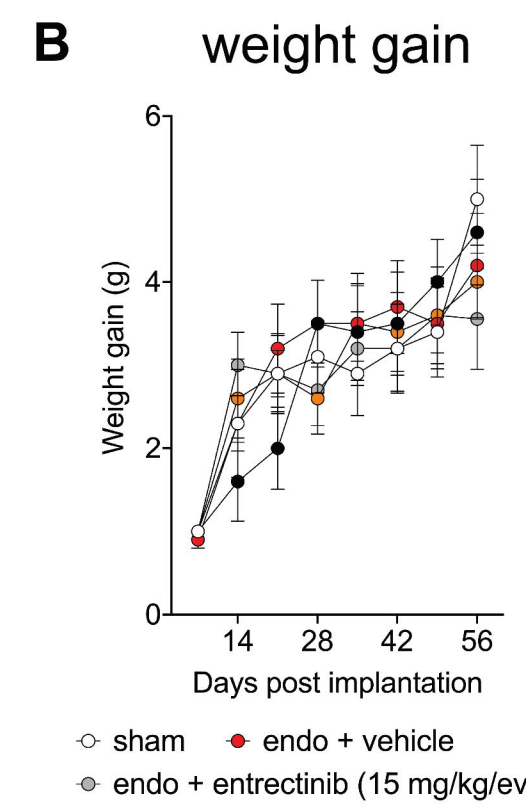
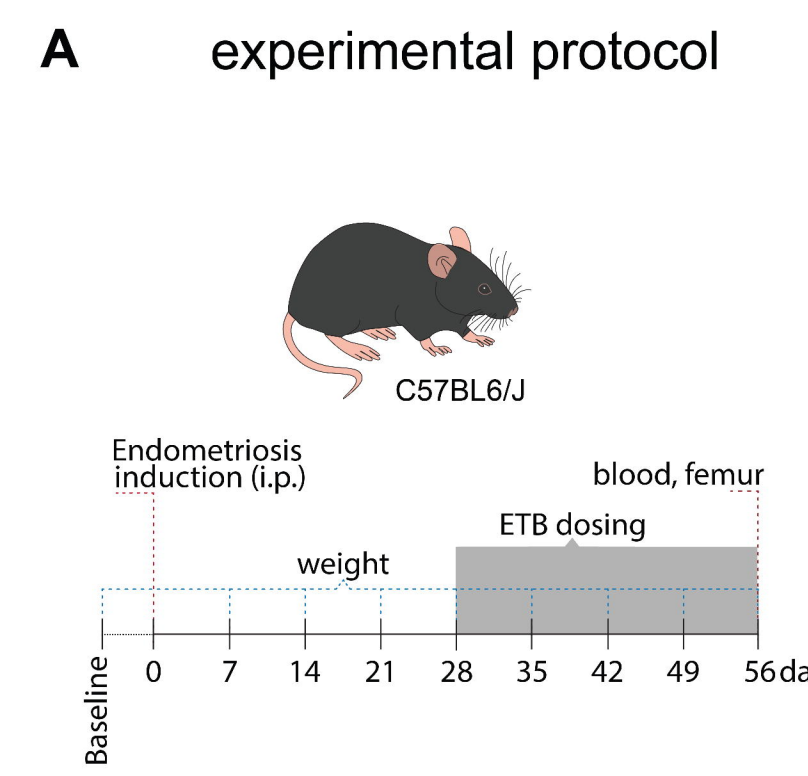
dorsal root ganglia



D

dorsal root ganglia





bone μCT analysis